

DEC 15 1989

PROPERTIES OF ALUMINUM-URANIUM ALLOYS (U)

AUGUST 1989

DO NOT MICROFILM
COVER

DOES NOT CONTAIN
UNCLASSIFIED CONTROLLED
NUCLEAR INFORMATION

Reviewing
Official:

C. J. Banick

C. J. Banick, Class Officer

Date

9/12/89

R.W. Benjamin
Derivative Classifier

Westinghouse Savannah River Company
Savannah River Site
Aiken, SC 29808

SAFETY • RESPONSIBILITY • SECURITY
SRS
SAVANNAH RIVER SITE

PREPARED FOR THE U.S. DEPARTMENT OF ENERGY UNDER CONTRACT DE-AC09-88SR18035

DISTRIBUTION OF THIS DOCUMENT IS UNLIMITED

DISCLAIMER

This report was prepared as an account of work sponsored by an agency of the United States Government. Neither the United States Government nor any agency thereof, nor any of their employees, makes any warranty, express or implied, or assumes any legal liability of responsibility for the accuracy, completeness, or usefulness of any information, apparatus, product, or process disclosed, or represents that its use would not infringe privately owned rights. Reference herein to any specific commercial product, process, or service by the trade name, trademark, manufacturer, or otherwise, does not necessarily constitute or imply its endorsement, recommendation, or favoring by the United States Government or any agency thereof. The views and opinions of authors expressed herein do not necessarily state or reflect those of the United States Government or any agency thereof.

DISCLAIMER

This report was prepared as an account of work sponsored by an agency of the United States Government. Neither the United States Government nor any agency thereof, nor any of their employees, makes any warranty, express or implied, or assumes any legal liability or responsibility for the accuracy, completeness, or usefulness of any information, apparatus, product, or process disclosed, or represents that its use would not infringe privately owned rights. Reference herein to any specific commercial product, process, or service by trade name, trademark, manufacturer, or otherwise does not necessarily constitute or imply its endorsement, recommendation, or favoring by the United States Government or any agency thereof. The views and opinions of authors expressed herein do not necessarily state or reflect those of the United States Government or any agency thereof.

DISCLAIMER

Portions of this document may be illegible in electronic image products. Images are produced from the best available original document.

WSRC-RP--89-489

DE90 003889

PROPERTIES OF ALUMINUM-URANIUM ALLOYS

Authors:

**H. B. PEACOCK
R. L. FRONTROTH**

Approved by:

**J. M. Stone
Manager, Materials Technology Section**

**R. W. Benjamin
Manager, Operational Planning**

Publication Date: August 1989

**Westinghouse Savannah River Company
Savannah River Site
Aiken, SC 29808**

DISTRIBUTION OF THIS DOCUMENT IS UNLIMITED

pe **MASTER**

Blank

**DO NOT MICROFILM
THIS PAGE**

ABSTRACT

Enriched aluminum-uranium alloys have been used for nuclear reactor fuel elements at the Savannah River Site (SRS) for over 30 years. The alloy also has been used for fuel in research and test reactors in the international community. Over 200,000 elements have been successfully irradiated at SRS without incident. No known accidents related to the fuel have occurred during irradiation with the exception of a few cladding penetrations due to localized corrosion.

Aluminum-uranium fuel elements are proposed for the New Production Reactor (NPR). To carry out design and study irradiation behavior, physical, mechanical and chemical properties were obtained from the literature and assembled into a manual so a consistent set of data are available.

Blank

**DO NOT MICROFILM
THIS PAGE**

A handwritten signature, possibly 'P', is located in the bottom right corner of the page.

CONTENTS

	PAGE
1. U-Al Alloy Fuel	
1.1 Introduction	1
1.2 History of UAl Alloy At SRS.....	1
2. Physical and Mechanical Properties	
2.1 Aluminum-Uranium Phase	7
2.2 Density.....	12
2.3 Thermal Conductivity.....	16
2.4 Thermodynamic Properties.....	20
2.5 Coefficient of Linear Expansion	20
2.6 Mechanical Properties.....	23
3. Chemical Properties	
3.1 Aluminum Fuel-Water Reactions	30
3.2 Irradiated Fuel-Water Reaction.....	30
3.3 Fuel-Steam Reactions	30
4. Irradiation Performance	
4.1 Irradiation Conditions.....	32
4.2 Microstructure.....	32
4.3 Swelling and Blister Threshold Temperature.....	36
5. In-Reactor Fuel Behavior	
5.1 Fuel Element Failures	41
5.2 Severe Accident Tests.....	41
6. Fission Product Release	
6.1 Gases and Volatiles.....	46
7. Fabricability	
7.1 Casting.....	49
7.2 Density Limit	49
7.3 Tube Fabrication and Production Yields.....	49
8. Reprocessing	
8.1 Physical Description.....	56
8.2 Process Description	56
8.3 Waste.....	57

v /ri

Blank

DO NOT MICROFILM
THIS PAGE

VI

LIST OF FIGURES

	PAGE
1 Savannah River Major Products.....	2
2 Thermal Neutron Flux For Optimum Production	3
3 Fuel Development to Match Power	6
4 Aluminum-Rich End of Equilibrium Phase Diagram for Al-U System.....	8
5 Typical Microstructure of Cast and Extruded 23.2 Wt.% U-Al Alloy.....	9
6 Typical Microstructure of Cast and Extruded 33.9 Wt.% U-Al Alloy.....	10
7 Typical Microstructure of Cast and Extruded 41.8 Wt.% U-Al Alloy.....	11
8 Composition vs Density of Al-U Alloys from 0 to 68.8 Wt. % Uranium.....	13
9 Relationships Between Composition, Density and % Volume of α - Aluminum - Uranium Alloy Structures	14
10 Effect of Composition on Thermal Conductivity at 65°C on Cast and Heat-Treated Aluminum-Uranium Alloys.....	17
11 Effect of Fission in Aluminum-Uranium Alloys Upon Ratio Of Final To Initial Thermal Resistivity.....	19
12 Heat Capacity Correlations for Aluminum and Uranium.....	21
13 Coefficient of Linear Thermal Expansion of 1100 Al and U-Al Alloys	22
14 Effect of Composition on the Mechanical Properties of Hot-Rolled Aluminum-Uranium Alloys.....	26
15 Microstructure of Cast Aluminum-Uranium Alloys Showing UA14 and UA13 Primary Phases.....	33
16 Photomicrographs of Irradiated Aluminum-Uranium Alloys	34
17 Irradiated and Annealed Aluminum - Uranium Alloys.....	35
18 Swelling of Irradiated Al-U (25 wt.%) Alloy During Annealing.....	38
19 Volume Increased Due to Cracks Formed During Annealing of Irradiated Al-25 wt.% U Alloy	39
20 Extent of Reaction of U/Al Plates with Water Resulting from Destructive Transient Irradiations	45
21 Comparisons of ORNL and SRL Data for U-Al Coupon Iodine Release	48
22 Extrusion Yields for High Wt. % Uranium-Aluminum	51
23 Flow Diagram for HWR Fuel Tube Fabrication Processes	52
24 Mark 16 Fuel Production Yield Data for 1978 - 1986	54
25 Mark 22 Fuel Production Yield Data for 1979 - 1987	55
26 Flow Diagram For Processing Irradiated Fuel to N _p O ₂ and UO ₃ (H Area).....	58

LIST OF TABLES

	PAGE
1 Demonstrated Operating Parameters	5
2 Uranium-Aluminum Alloy Constants Used in SRS Computer Codes.....	15
3 Thermal Conductivity of Aluminum-Uranium Alloys	18
4 Coefficient of Linear Expansion of Aluminum-Uranium Alloys	24
5 Mechanical Properties of Aluminum-Uranium Alloys.....	25
6 Tensile Properties of Forged Aluminum-Uranium Alloys	27
7 High-Temperature Properties of Aluminum-Uranium Alloys	28
8 Worst Case Consequences Attending Presumed Cooling System Failures	42
9 Quantities Used in Heat Calculations	43
10 Extrusion Yields of High Uranium Concentration Mark 16 Outer Tubes	50

Blank

**DO NOT MICROFILM
THIS PAGE**

1.0 ALUMINUM-URANIUM ALLOYS

1.1 Introduction

Aluminum-uranium alloys that are clad with aluminum are particularly attractive as fuels for low-temperature, water-cooled and water-moderated reactors. Aluminum has good thermal conductivity and has a low capture cross section for thermal neutrons. Both properties make aluminum the choice material for Savannah River Site (SRS) reactor fuel assemblies.

Reactor fuel elements contain enriched uranium in the fuel core section, sometimes called the meat, and are clad with 8001 aluminum alloy. Cast aluminum-uranium alloys have been used for the core section of fuel elements at SRS for about 30 years. Enriched uranium is obtained from Oak Ridge and alloyed with aluminum at Savannah River. The alloy is cast into graphite molds, and the casting is extruded to form a log. The log is machined into billet cores for a second extrusion operation. Billet cores are placed inside 8001 aluminum components and coextruded to produce aluminum clad tubes about fifteen-feet long.

During the years of SRS operation, the inventory of uranium has been recycled through the reactors. This was done to minimize the need for drawing virgin or alloy from the weapons stockpile. This policy adds 236U to the recycle inventory and has resulted in a gradual increase in the total amount of uranium needed in each fuel assembly to maintain the effective 235U required for operation. The uranium content in fuel tubes has gradually increased to 33 weight percent uranium. Because of low power operation of the SRS reactors at the present time, and the projected availability of ICPP uranium, the total uranium content in reactor assemblies should be reduced for future operations as the 236U is diluted in a larger uranium inventory.

There is a long history of UAl alloy use as a fuel for manufacture of isotopes other than tritium and plutonium in the SRS reactors. A summary of this history is included to show the depth of experience that is available with this fuel form. This information combined with physical and mechanical property data are included from published reports to aid in selection and design of the fuel for the New Production Reactor (NPR).

1.2 History of UAl Alloy at SRS

Several products have been produced at SRS since start up of the reactors in 1954. An unclassified summary of the products and quantity produced is shown in Figure 1. Although weapon materials have been the primary product of the site, materials have also been produced for space missions and for medical applications.

Each of the reactor products require a specific reactor lattice design to achieve optimum production of the desired isotopes. In some cases where two or more products are desired, the reactor has been configured with a mixed lattice design which utilizes both fuel and target materials positioned for effective irradiation in the reactor core. The aluminum-uranium cast and extruded fuel has been used for these applications. Concentric tubes with varying tube wall thicknesses and uranium loading have been used for reactor fuel elements for about thirty years.

Figure 2 shows the range and levels of thermal neutron flux required to produce various isotopes. The very high flux level was achieved by using thin core fuel

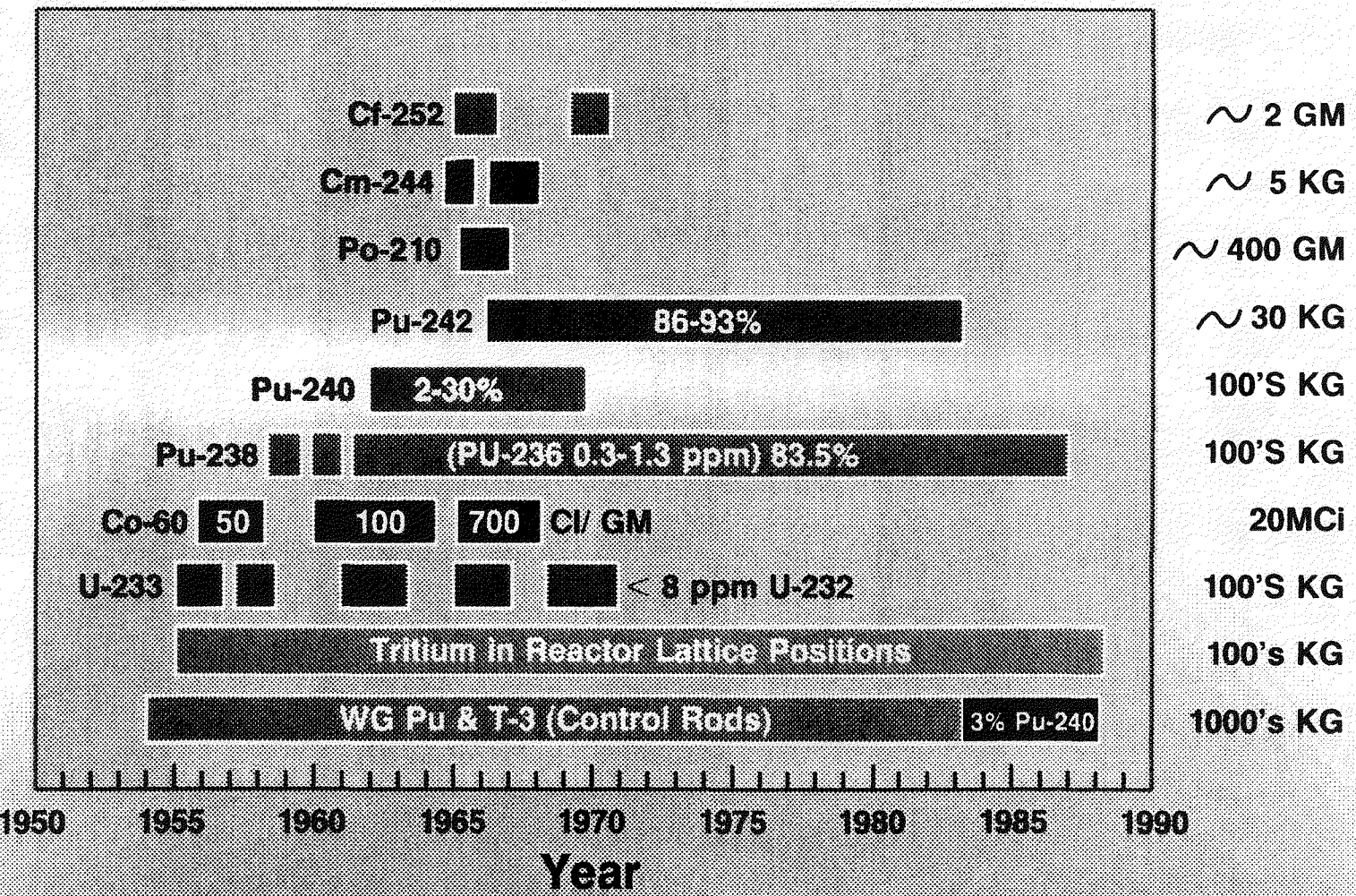


FIGURE 1. SAVANNAH RIVER MAJOR PRODUCTS

0002946.01

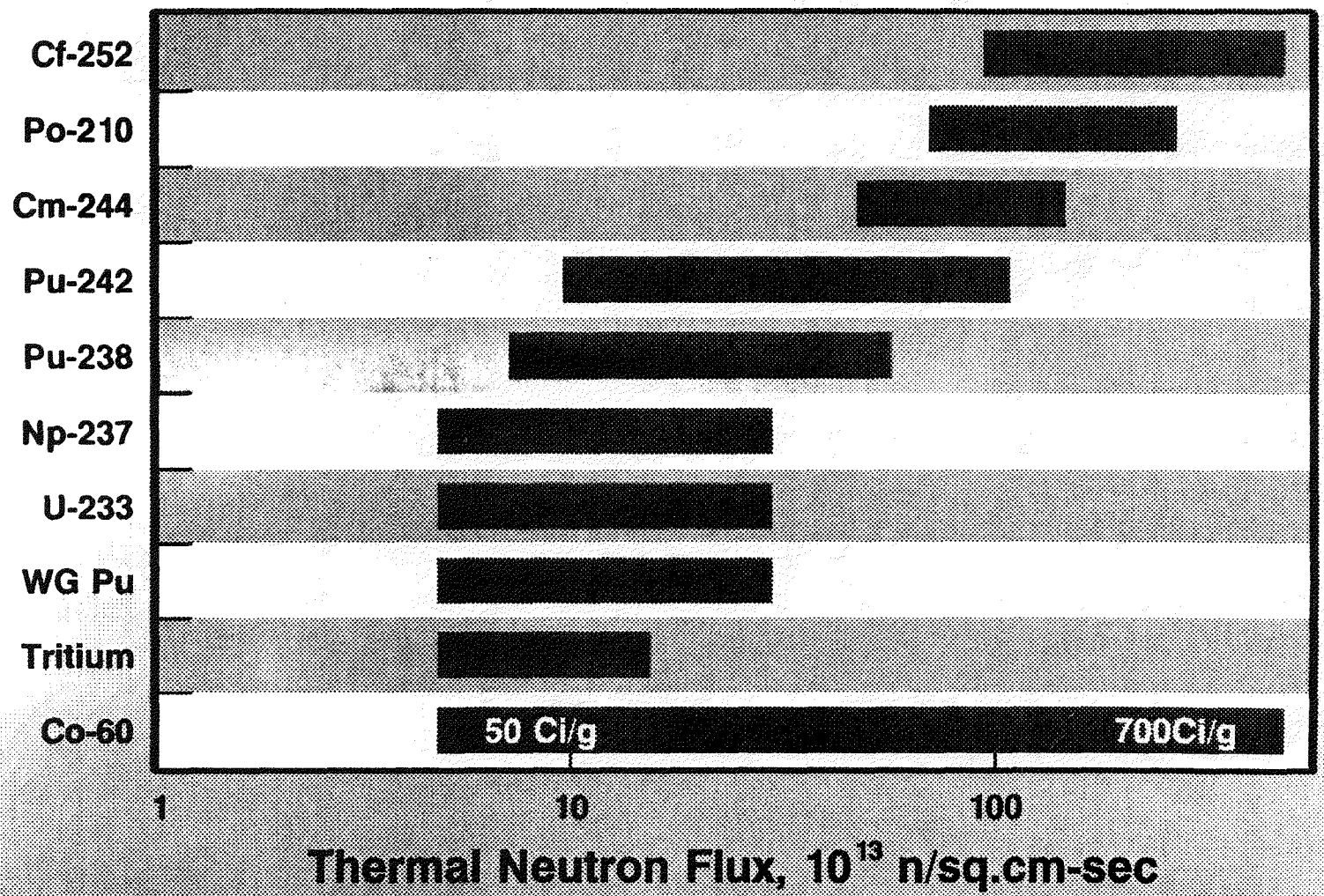


FIGURE 2. THERMAL NEUTRON FLUX FOR OPTIMUM PRODUCTION

concentrated in the center of the reactor. Thin wall tubes permitted adequate cooling of the assembly during the irradiation cycle.

As shown in this report, aluminum has many advantages for material production reactors. Unlike power producing reactors, the fuel and target assemblies are charged and discharged regularly on a rapid recharging schedule. For this reason aluminum offers advantages in that it is easily fabricated using standard casting and metal working methods when alloyed with uranium. Uranium and aluminum are very compatible with each other. Aluminum is inexpensive compared to other materials that are used in power producing reactors and has very low corrosion rates when temperatures are kept below ~ 150 $^{\circ}\text{C}$. In the reactor, aluminum has very good strength at operating temperatures and it helps the environment by being an excellent tritium and fission gas barrier. As a final tribute to the characteristics of aluminum, it is easy to dissolve, permitting easy recycle of uranium within the SRS processing cycle.

The reactor charge design is modified for each of the special products, as consideration is given to product half life, fission and capture cross sections; and fuel loadings, power, and location in relation to the special targets required for the product. In each case aluminum-uranium alloy was the basic material in the fuel assemblies, using an aluminum alloy cladding. The basic considerations given to design of fuel assemblies were dependent upon several factors. As already mentioned reactor flux levels must change based upon the products being produced. This immediately impacts the sizes and shapes of the elements placed in the reactor. Irradiation performance and productivity are matched with the potential of the reactor hydraulic system. Risk to the environment and the amount of waste that is generated throughout the processing life of the materials have been given top consideration. Appendix 1 gives sketches of the SRS reactor lattice and the present fuel and target assemblies used in the reactors. The designation Mark 16 assembly is made up of two enriched tubes and two Li-Al tubes for production of tritium, with Mark 31 assemblies containing depleted uranium slugs for producing plutonium. The Mark 16 and Mark 31 assemblies are placed in the reactor in a mixed lattice arrangement as compared to a homogeneous arrangement for Mark 22 assemblies. Mark 22 assemblies are used for producing tritium alone. The demonstrated operating parameters of U-Al and reactor power attained for each fuel design are shown in Table 1 and Figure 3.

TABLE I

Demonstrated Operating Parameters

(Extreme for Low and High Neutron Flux)

<u>Parameter</u>	<u>High Flux</u>	<u>Low Flux</u>
Thermal Neutron Flux, $n/cm^2/sec$	6.1×10^{15}	9×10^{13}
Reactor Power, MW	800	2900
Max Fuel Assembly Power, MW	21	~7
Max Fuel Heat Flux, BTU/HR/ft ²	2.5×10^6	1×10^6
Max Fuel Coolant Velocity, ft/sec	70	25
Fuel Cycle Length, days	4	200 - 350
Fuel Burnup (Avg), %	26	45 - 70

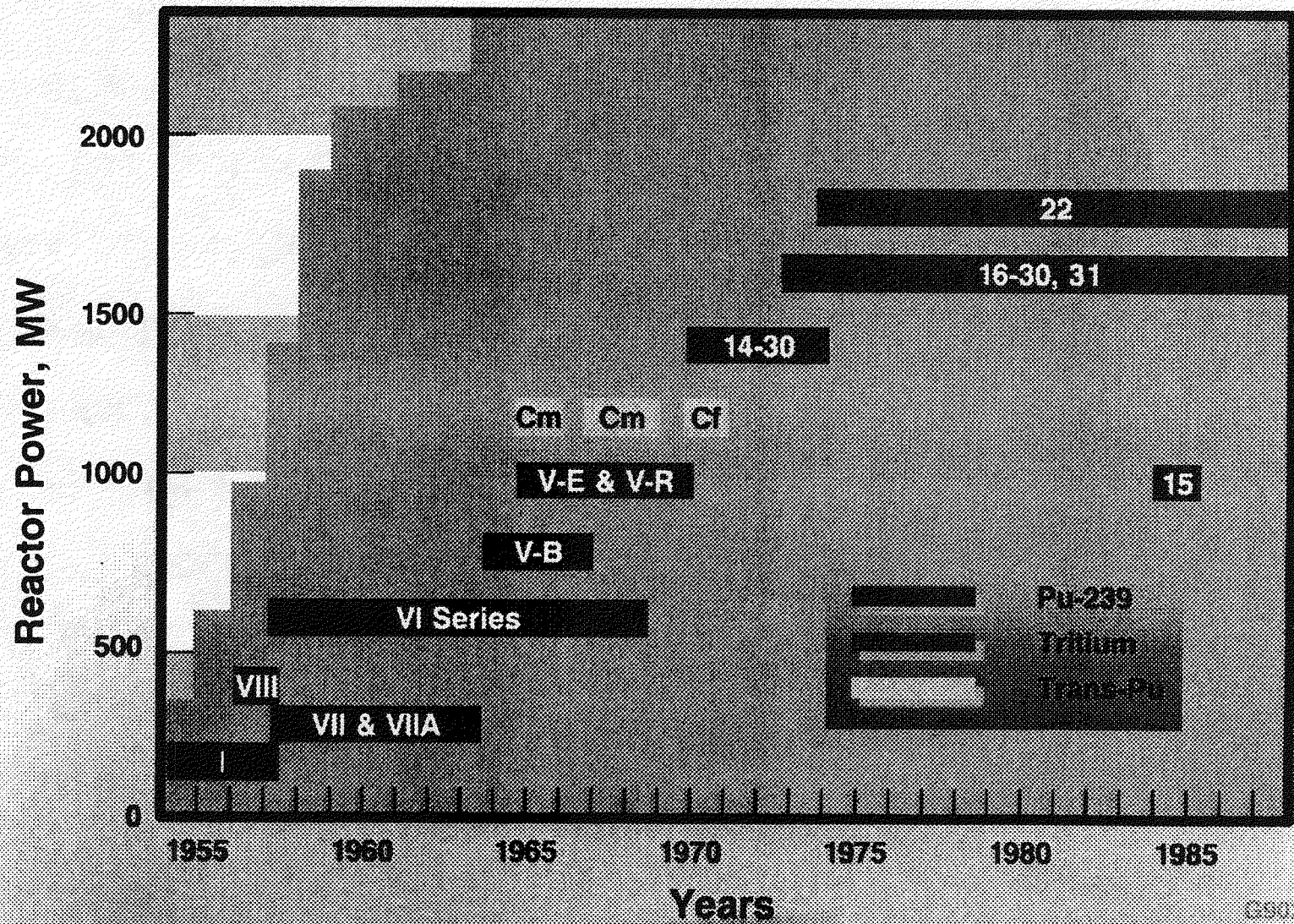


FIGURE 3. FUEL DEVELOPMENT TO MATCH POWER

2.0 PHYSICAL AND MECHANICAL PROPERTIES

2.1 Aluminum-Uranium Phases

Compositions of less than about 40 wt% uranium in aluminum are of interest for fuel element fabrication. Above 35 wt% uranium, fabricability becomes difficult and at 40 wt% it is almost impossible to manufacture tubes by extrusion. Fabricability depends on the phases present which effect the physical and mechanical properties of the alloy.

The aluminum-uranium equilibrium phase diagram^{1,2} is used to determine phases formed during equilibrium cooling of an alloy. Although equilibrium conditions can not be achieved in a normal production casting, this diagram serves to predict phases that may be present. Generally, a casting has a higher cooling rate. This, in effect, alters reaction temperatures which changes the relative amounts of the various phases present in the microstructure. Phases in the alloy also depend upon the composition and homogeneity of the alloy, and on its heat treatment.

The solubility of uranium in aluminum is generally considered negligible³. However, Jones, Street, Scoberg and Baird⁴ reported a solubility of 0.06 wt% uranium at the eutectic temperature of about 920°K (647°C). A revised equilibrium phase diagram by Mondolfo⁵ is shown in Figure 4 for alloy contents up to 80 wt% uranium.

The liquidus temperature, or the temperature when an alloy is completely molten, depends on the uranium composition. Aluminum melts at about 933°K (660°C). The liquidus of the alloy gradually decreases to 920°K (647°C) as the uranium content increases to 13.2 wt% uranium, the eutectic composition. Above the eutectic composition, the liquidus temperature increases with uranium content until the intermetallic compound UAl_2 is formed at a composition of approximately 81 wt% uranium. As the uranium content continues to increase, the liquidus temperature decreases.

The phase diagram predicts that at equilibrium a composition of basically pure aluminum and the intermetallic compound UAl_4 exists below 920°K for alloys containing less than 64.2 weight percent uranium in aluminum. At 13.2 wt% uranium and 920°K, an eutectic reaction occurs producing a mechanical mixture of about 80.6% aluminum and 19.4% UAl_4 . Increasing temperature, increases the solubility of uranium in molten aluminum. A peritectic reaction occurs at about 1000°K between liquid and solid UAl_3 to form UAl_4 . At 1623°K another peritectic reaction occurs between the liquid and UAl_2 to form the compound UAl_3 . The UAl_2 intermetallic compound forms from the liquid at about 1895°K.

Casting of 30-40 wt% aluminum-uranium alloys exhibit primary aluminides of both UAl_3 and UAl_4 . The relative amounts of each phase present depends on the cooling rate of the cast alloy. Nonequilibrium microstructures of cast and extruded alloys with different concentrations of uranium are shown in Figures 5, 6 and 7.

The reaction between UAl_3 and liquid to form UAl_4 can be inhibited by the addition of alloying elements which stabilizes the UAl_3 compound. Thurber and Beaver⁶ have shown that small amounts (3 wt%) of silicon, zirconium, germanium, titanium or tin suppress the formation of UAl_4 .

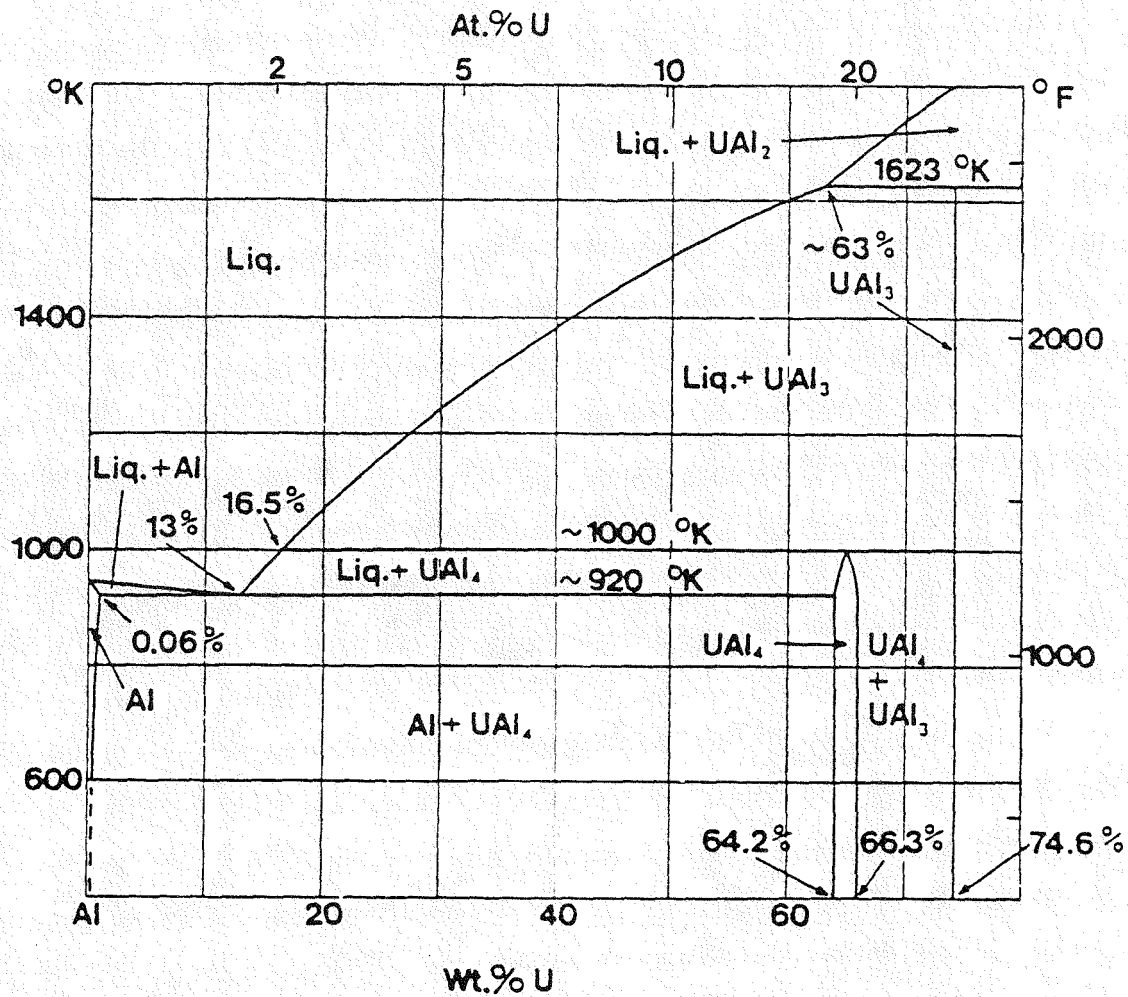


FIGURE 4. ALUMINUM-RICH END OF EQUILIBRIUM PHASE DIAGRAM FOR AL-U SYSTEM

Reference: Mondolfo, L. F., Aluminum Alloys: Structure and Properties, Butterworth & Co. (Publishers) Ltd., London (1976).



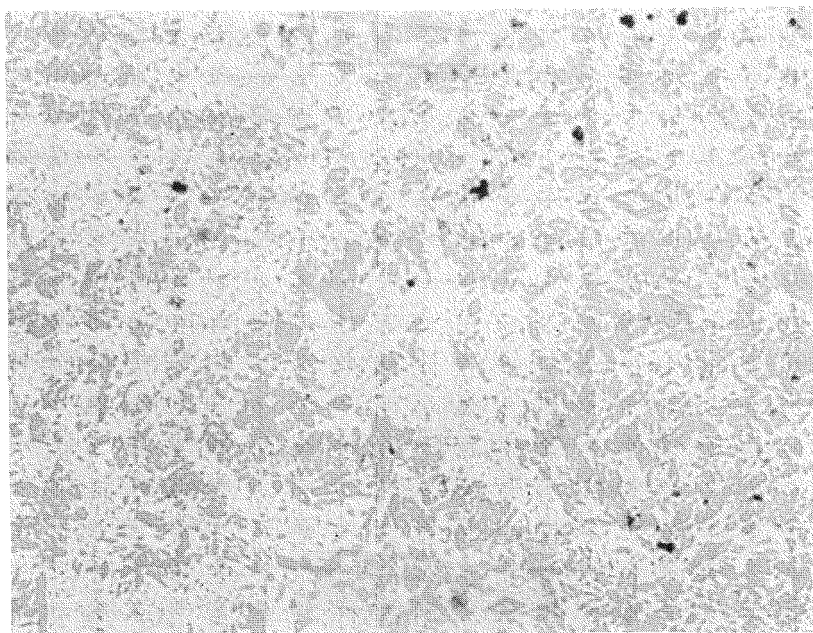
100X

Neg No. 55425-M

Composition - 23.2 wt % U-Al
Phase distribution (QMS Analysis)

15.6 Volume % Aluminum
11.5 Volume % Primary Aluminide ($UA1_4$)
71.8 Volume % Eutectic
Area of Average Primary Aluminide Particle - 260 Sq. Microns
Area of Average Aluminum Particle - 158 Sq. Microns

FIGURE 5. TYPICAL MICROSTRUCTURE OF CAST AND EXTRUDED 23.2 WT % U-AL ALLOY

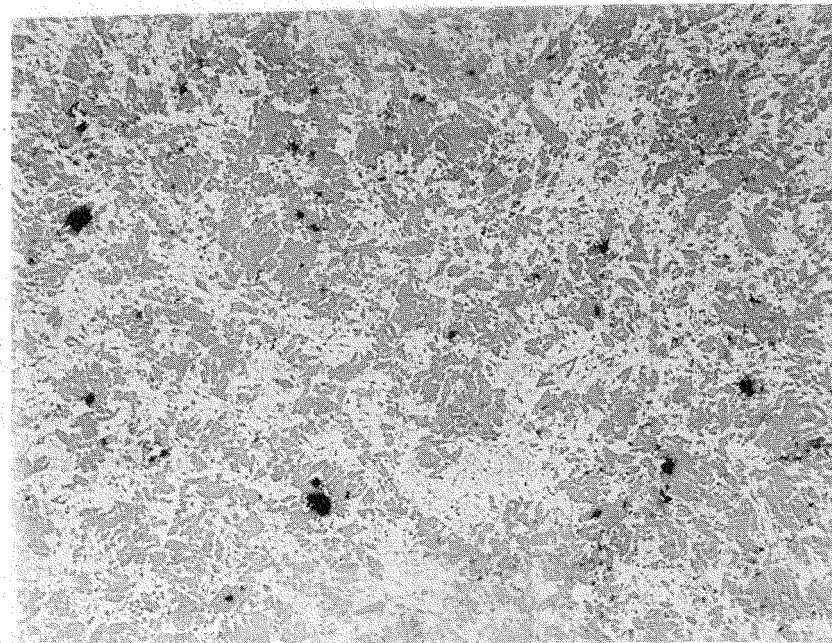


100X

Neg No. 55426-M

Composition - 33.9 wt % U-Al
Phase distribution (QMS Analysis)
56.1 Volume % Aluminum
28.9 Volume % Primary Aluminide (UAl_4 , UAl_3)
15.0 Volume % Eutectic
Area of Average Primary Aluminide Particle - 196 Sq. Microns
Area of Average Aluminum Particle - 1903 Sq. Microns

**FIGURE 6. TYPICAL MICROSTRUCTURE OF CAST AND EXTRUDED
33.9 WT % U-AL ALLOY**



100X

Neg No. 55427-M

Composition - 41.8 wt % U-Al

Phase distribution (QMS Analysis)

38.2 Volume % Aluminum (dendritic + eutectic)

37.5 Volume % Primary (UAl₄, UAl₃)

71.8 Volume % Eutectic Aluminide (UAl₄)

Area of Average Primary Aluminide Particle - 309 Sq. Microns

Area of Average Aluminum Particle - 477 Sq. Microns

FIGURE 7. TYPICAL MICROSTRUCTURE OF CAST AND EXTRUDED 41.8 WT % U-AL ALLOY

2.2 Density

Crystal structure of UAl_4 was determined by Borie⁷ using X-ray diffraction. The intermetallic compound has a body-centered orthorhombic unit cell with lattice parameters $a = 4.41\text{\AA}$, $b = 6.27\text{\AA}$ and $c = 13.71\text{\AA}$ where \AA indicates units in angstroms. The crystal structure of UAl_3 is simple cubic with $a = 4.26\text{\AA}$ whereas the structure of UAl_2 is face-centered cubic with $a = 7.72\text{\AA}$.

The density of the compounds UAl_4 and UAl_3 has been calculated using X-ray data. Kaufmann and Gordon⁸ reported the density of UAl_4 to be 6.06 gm/cc and the density of UAl_3 to be 6.80 gm/cc. Borie measured the density of UAl_4 and found it to be 5.7 ± 0.3 gm/cc with a compositional range of 64.2 to 66.3 wt% uranium.

The density of aluminum-uranium alloys was calculated by Aronin and Klein⁹. The density is shown in Figure 8 for alloys containing up to about 68 wt% uranium. Aronin et al. compared calculated uranium content data using density relationships with analytical data obtained from chemical analysis of the samples. The calculated uranium content was well within the uncertainty of the chemical analysis data which was reliable to $\pm 1\%$ of the uranium content for alloys containing 7 to 21 % uranium.

The density of alloys containing up to about 68 wt% uranium can be described by the empirical equation $\rho = 3.3502/(1.2408 - X)$, where X is the weight fraction of uranium¹⁰. The equation is valid if (1) high-purity aluminum is used; (2) all the uranium is present as UAl_4 ; and (3) there are no voids. Above about 25 wt% uranium, the presence of nonequilibrium UAl_3 and voids change the relationship.

Jones et al.⁴ cast aluminum-uranium alloys to measure the thermal conductivity as described in the next section. Density measurements were made on machined samples. Good agreement was found between the measured and estimated densities for alloys containing up to 42 wt% uranium. Results are shown in Figure 9. Estimates were based on the densities and the volumes of α -aluminum and UAl_4 that would be present in the alloys under equilibrium. These estimates were made using 5.7 gm/cc for UAl_4 which was determined by Borie. Comparison of the data with Aronin et al's calculated data indicates good agreement for aluminum-uranium alloys containing less than about 40 wt % uranium.

Density and other physical constants for U-Al alloys used in SRS reactor calculations are given in Table II

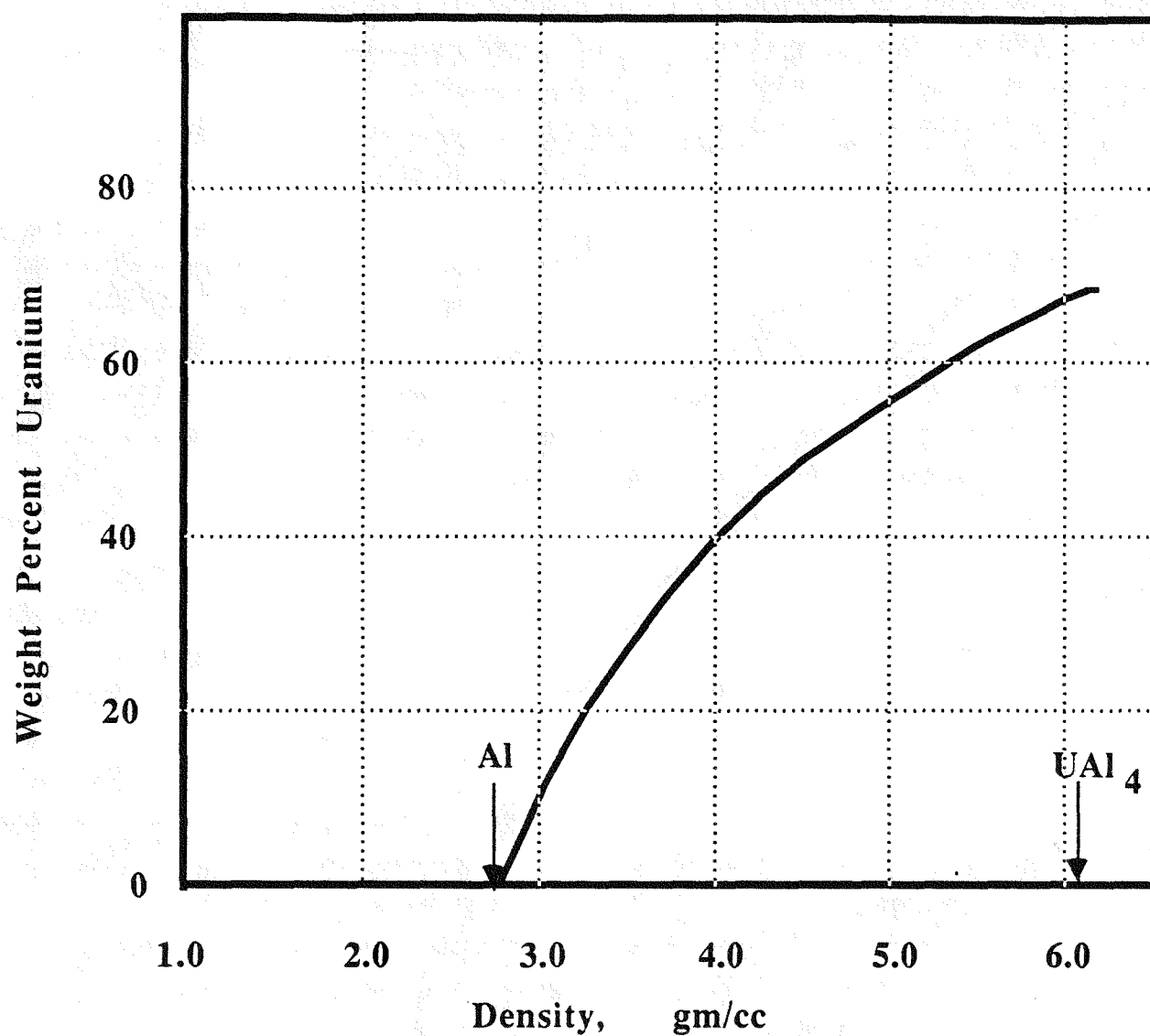


FIGURE 8. COMPOSITION VS DENSITY OF AL-U ALLOYS FROM 0 TO 68.8 WT PERCENT URANIUM

Reference: Aronin, L.R., and Klein, J.L., "Use of a Density (Specific Volume) Method as a Sensitive Absolute Measure of Alloy Composition, and its Applications to the Aluminum-Uranium System," Nuclear Metals, Inc. NMI-1118, 1954

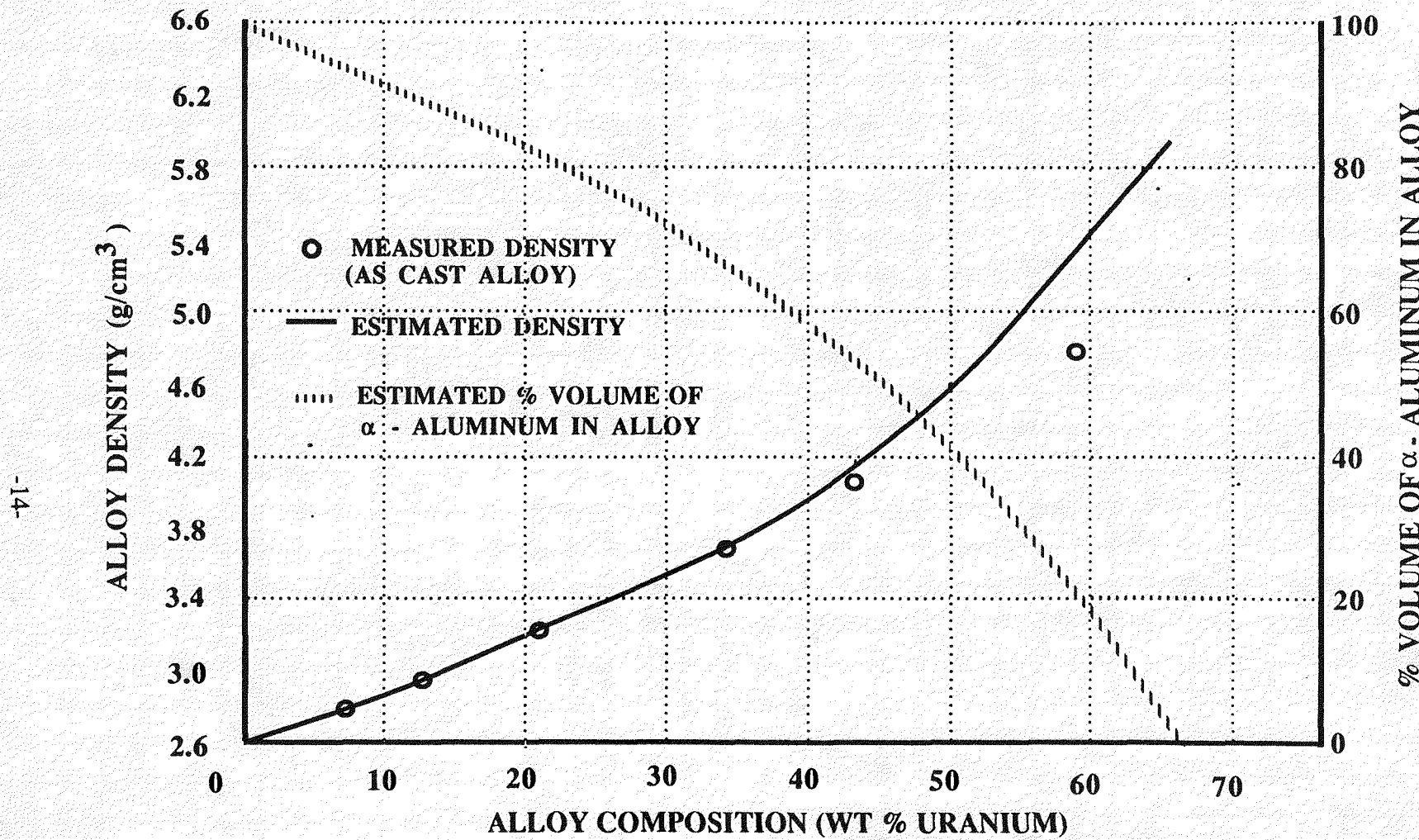


FIGURE 9. RELATIONSHIPS BETWEEN COMPOSITION, DENSITY AND % VOLUME OF α -ALUMINUM-URANIUM ALLOY STRUCTURES

REFERENCE: Jones, T.I., Street, K.N., Scobey, J.A. and Baird, J., "Relationship Between Microstructure and Thermal Conductivity in Aluminum-Uranium Alloys," Can. Met. Quarterly, pp 53-72, 1963.

TABLE II
URANIUM-ALUMINUM ALLOY CONSTANTS
USED IN SRS COMPUTER CODES

Weight Percent Uranium	Density Alloy gm/cc	gm U/cc	gm Al/cc	gm Al/cc Al in UAl	gm Al/cc free Al	cc Al/cc Alloy	ccU/cc Alloy
1	2.7219	.0272	2.6947	.0125	2.6822	.9854	.0146
2	2.7441	.0549	2.6892	.0252	2.6640	.9708	.0292
3	2.7667	.0830	2.6837	.0381	2.6456	.9562	.0438
4	2.7897	.1116	2.6781	.0513	2.6268	.9416	.0584
5	2.8131	.1407	2.6724	.06467	2.6077	.9269	.0731
6	2.8368	.1702	2.6666	.0782	2.5884	.9124	.0876
7	2.8610	.2003	2.6607	.0921	2.5686	.8977	.1023
8	2.8855	.2308	2.6547	.1061	2.5486	.8832	.1168
9	2.9105	.2619	2.6486	.1204	2.5282	.8686	.1314
10	2.9360	.2936	2.6424	.1349	2.5075	.8540	.1460
11	2.9619	.3258	2.6361	.1497	2.4864	.8394	.1606
12	2.9882	.3586	2.6296	.1648	2.4648	.8248	.1752
13	3.0150	.3920	2.6230	.1802	2.4428	.8102	.1898
14	3.4023	.4259	2.6164	.1957	2.4207	.7956	.2044
15	3.0701	.4605	2.6096	.2116	2.3980	.7810	.2190
16	3.0984	.4957	2.6027	.2278	2.3749	.7664	.2336
17	3.1273	.5316	2.5957	.2443	2.3514	.7518	.2482
18	3.1567	.5682	2.5885	.2611	2.3274	.7372	.2628
19	3.1866	.6055	2.5811	.2783	2.3028	.7226	.2774
20	3.2171	.6434	2.5737	.2957	2.2780	.7080	.2920
21	3.2482	.6821	2.5661	.3135	2.2526	.6934	.3066
22	3.2799	.7216	2.5583	.3316	2.2267	.6788	.3212
23	3.3123	.7618	2.5505	.3501	2.2004	.6643	.3357
24	3.3453	.8028	2.5425	.3690	2.1735	.6497	.3503
25	3.3789	.8447	2.5342	.3882	2.1460	.6351	.3649
26	3.4132	.8874	2.5258	.4078	2.1180	.6205	.3795
27	3.4482	.9310	2.5172	.4279	2.0893	.6059	.3941
28	3.4840	.9755	2.5085	.4483	2.0602	.5913	.4087
29	3.5205	1.0209	2.4996	.4692	2.0304	.5767	.4233
30	3.5578	1.0673	2.4905	.4905	2.0000	.5621	.4379
31	3.5959	1.1147	2.4812	.5123	1.9689	.5475	.4525
32	3.6348	1.1631	2.4717	.5346	1.9371	.5329	.4671
33	3.6746	1.2126	2.4620	.5573	1.9047	.5183	.4817
34	3.7152	1.2631	2.4521	.5805	1.8716	.5037	.4963
35	3.7567	1.3148	2.4419	.6043	1.8376	.4891	.5109
36	3.7992	1.3677	2.4315	.6286	1.8029	.4770	.5230
37	3.8427	1.4218	2.4209	.6535	1.7674	.4599	.5401
38	3.8871	1.4771	2.4100	.6789	1.7311	.4453	.5547
39	3.9326	1.5337	2.3989	.7049	1.6940	.4307	.5693
40	3.9792	1.5917	2.3875	.7315	1.6560	.4161	.5839

2.3 Thermal Conductivity

Thermal conductivity is a material property which indicates the quantity of heat that will flow across a unit area if the temperature gradient is unity. In general, the value of the thermal conductivity varies with temperature and alloy additions.

The addition of uranium to aluminum lowers the thermal conductivity. In fact, the thermal conductivity of Al-30.5 wt% uranium alloy is about 70% of the thermal conductivity of pure aluminum. Pure aluminum has a conductivity about five times greater than pure uranium.

Measurements of the thermal conductivity at 65°C were made by Jones, et. al⁴ on aluminum alloys containing up to 58 wt% uranium in the as-cast and heat-treated conditions. The measured conductivity varied from $0.541 \text{ cal sec}^{-1} \text{ cm}^{-2} \text{ }^{\circ}\text{C}^{-1} \text{ cm}$ for a pure aluminum extruded rod to $0.081 \text{ cal sec}^{-1} \text{ cm}^{-2} \text{ }^{\circ}\text{C}^{-1} \text{ cm}$ for a heat-treated alloy containing 58 wt% uranium. Changes in thermal conductivities, produced by heat treatments, were related to corresponding changes in the microstructure. The thermal conductivity of UAl_4 and UAl_3 was found to be $0.02 \text{ cal sec}^{-1} \text{ cm}^{-2} \text{ }^{\circ}\text{C}^{-1} \text{ cm}$ by extrapolating the data. Figure 10 shows the effect of composition on the thermal conductivity at 65°C for cast and heat-treated aluminum-uranium alloys.

Alloys containing large quantities of UAl_3 lowered the conductivity when UAl_3 transformed to UAl_4 during heat treatment. This was attributed to (1) the increased volume of the intermetallic phase in the structure and (2) reduced volume of aluminum in the structure. From stoichiometric calculations, the volume is expected to increase about 7% for the reaction.

Thermal-conductivity measurements were reported by Saller¹⁰ at 200, 300 and 400°C for forged bars containing 12.5, 22.7 and 30.5 weight percent uranium. All samples were annealed 1/2 hour at 370°C prior to testing. Tests were conducted using the United States Bureau of Standards method given in Research Paper RP668, April 1934. Results for the aluminum-uranium alloys as well as for pure aluminum and uranium are tabulated in Table III as a function of temperature. Temperature has a small effect on the thermal conductivity of aluminum-uranium alloys in the 200-400°C temperature range.

Irradiation decreases the thermal conductivity^{11,12,13} of aluminum-uranium alloys. Thermal resistivity is considered the reciprocal of conductivity. A plot of the effect of atoms fissioned on the ratio of final to initial thermal resistivity (R_f/R_i) is shown in Figure 11. As the fraction of total atoms fissioned increased to 6×10^{-3} , the ratio of the thermal resistivity increased to about 1.5, a 50% increase. This is equivalent to a burnup of 0.6%.

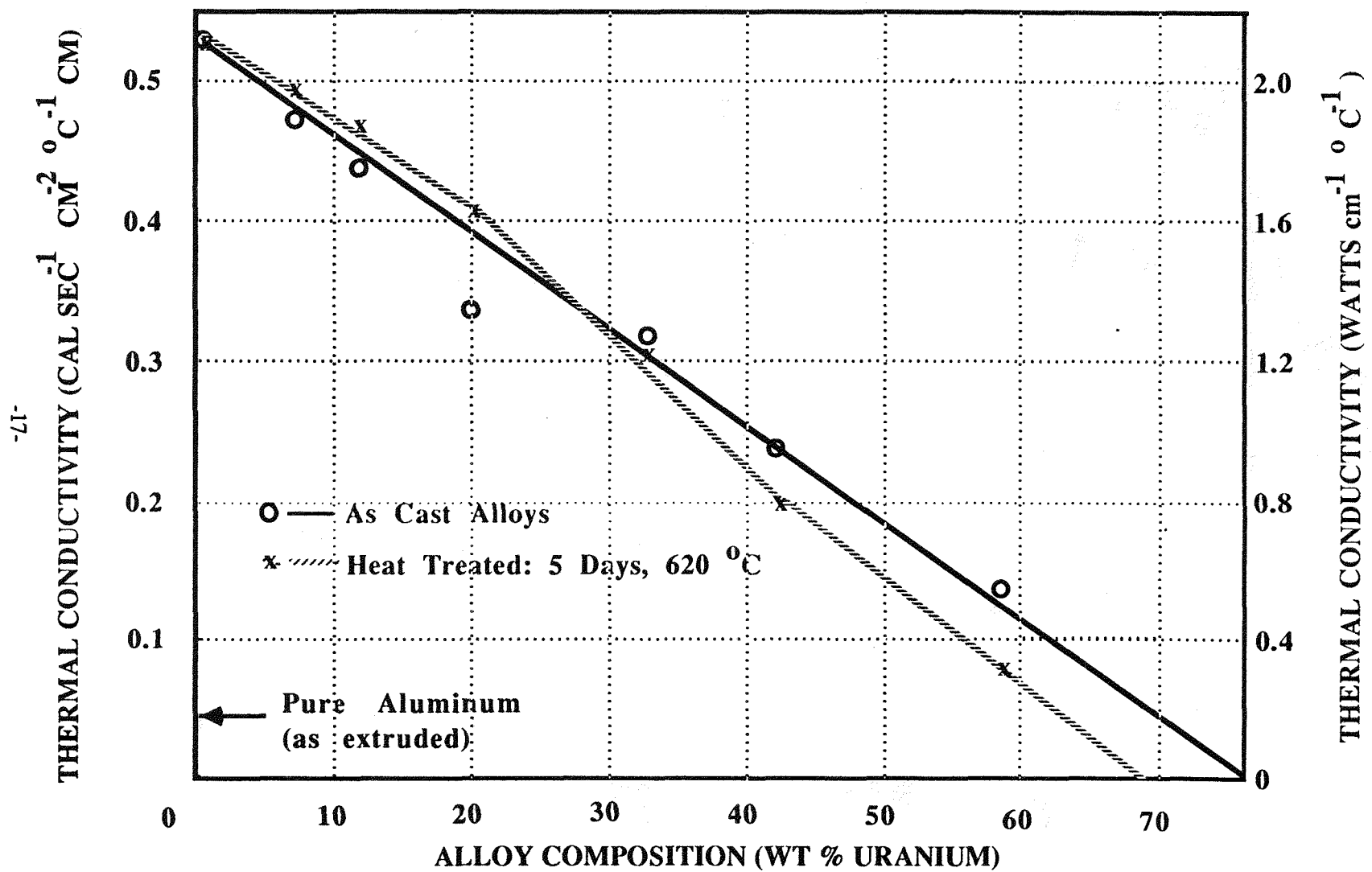


FIGURE 10. EFFECT OF COMPOSITION ON THERMAL CONDUCTIVITY AT 65 $^{\circ}\text{C}$ ON CAST AND HEAT-TREATED ALUMINUM-URANIUM

REFERENCE: Jone, T.I., Street, K.N., Scoberg, J.A., Baird, J. "Relationship Between Microstructure and Thermal Conductivity in Aluminum-Uranium Alloys, Can. Met. Quart., V-2, pp 53-72, 1963

TABLE III
THERMAL CONDUCTIVITY OF ALUMINUM-URANIUM ALLOYS

Uranium content, wt. %	Thermal conductivity, watts/cm ² /°C/cm (cal sec ⁻¹ cm ⁻² °C ⁻¹ Cm)		
	At 200°C	At 300°C	At 400°C
0	2.19 (0.52)	2.25 (0.54)	2.31 (0.55)
12.5	1.83 (0.44)	1.81 (0.43)	1.79 (0.43)
22.7	1.68 (0.40)	1.64 (0.39)	1.59 (0.38)
30.5	1.51 (0.36)	1.49 (0.36)	1.48 (0.35)
100	0.29 (0.07)	0.31 (0.07)	0.33 (0.08)

Reference: Saller, H. A. "Preparation, Properties and Cladding of Aluminum-Uranium, Alloys", Proceedings of the International Conference on the Peaceful Uses of Atomic Energy, Vol. 9, P/562, p214, United Nations, NY, 1956.

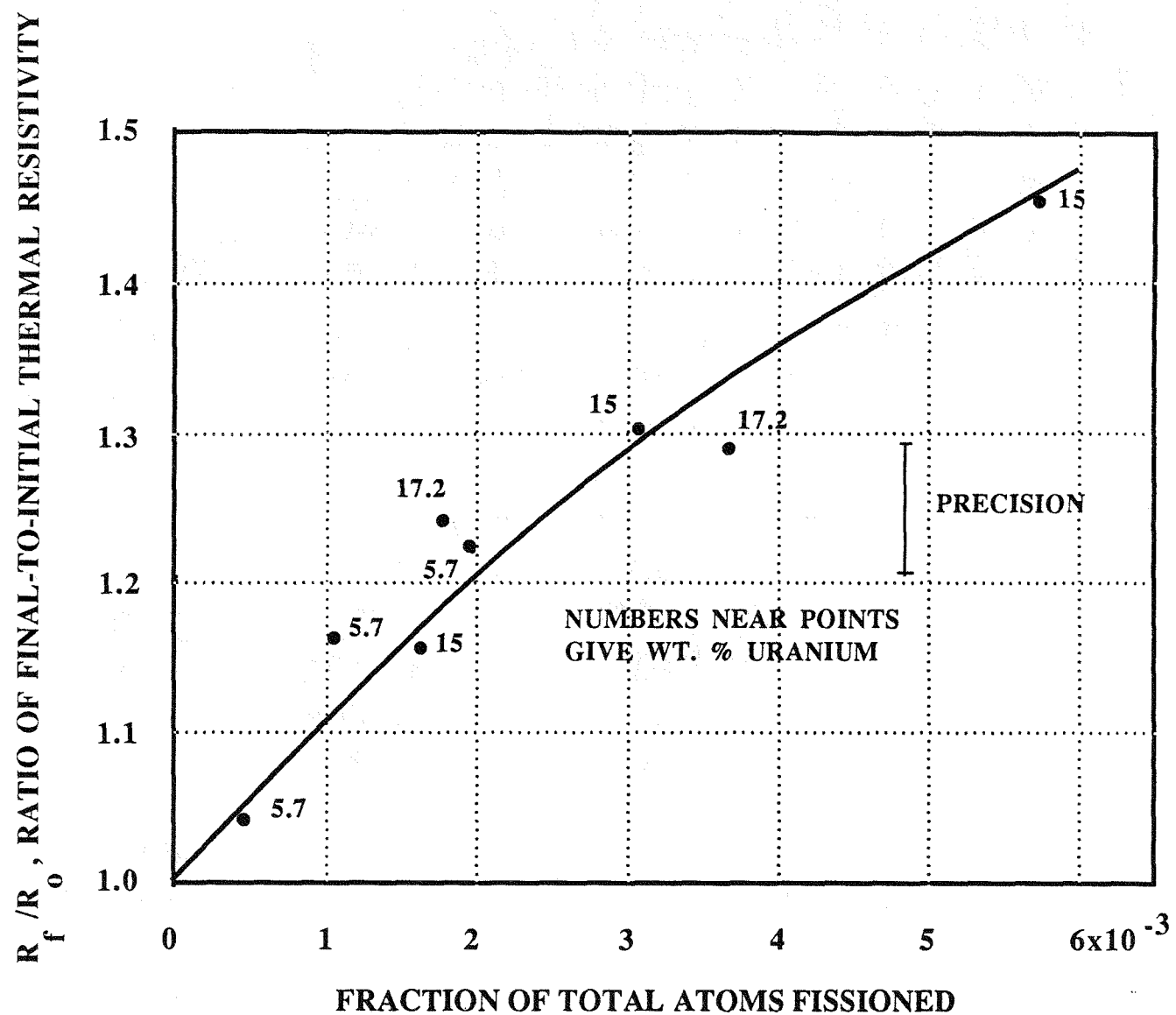


FIGURE 11. EFFECT OF IRRADIATION ON ALUMINUM-URANIUM ALLOYS UPON RATIO OF FINAL TO INITIAL THERMAL RESISTIVITY

REFERENCE: Billington, D.S., and Crawford, Jr., J.H., "Radiation Damage in Solids," Princeton University Press, 1961

2.4 Thermodynamic Properties

ENTHALPY

The enthalpy of uranium to 1500°K was determined by Marchidan et. al. by drop calorimetry¹⁴. From the experimental results, six polynomial equations were smoothed for the enthalpy of uranium. Analysis of the experimental enthalpy revealed transitions near 940, 1048 and 1405°K. The results obtained for enthalpies of transitions were: $U\alpha = U\beta, \Delta H = (2556 \pm 75) \text{ J mol}^{-1}$; $U\beta = U\gamma, \Delta H = (4182 \pm 85) \text{ J mol}^{-1}$; $U_l = U_{\text{liquid}}, \Delta H = (6979 \pm 120) \text{ J mol}^{-1}$. An equation was derived for the heat capacity. Derived thermodynamic functions for uranium are tabulated at every 50°K from 300 to 1500°K.

FREE ENERGY

The enthalpy of formation of U-Al compounds and the peritectic decomposition of UAl_4 was measured using an adiabatic calorimeter¹⁵. The enthalpies of formation at 298 K for the three compounds UAl_4 , UAl_3 and UAl_2 were determined to be 29.8, 25.9, and 22.1 kcal/mole, respectively. The uncertainty in the measurements were ± 2.0 kcal/mole. These data were combined with emf data, taken over a temperature range of about 400 to 700°C, to give thermodynamic relations for the compounds. The free energy relationships developed were:

$$\begin{aligned} G^\circ(\text{UAl}_4) &= -32,040 - 7.52T \ln T + 59.07T \\ G^\circ(\text{UAl}_3) &= -26,290 - 1.305T \ln T + 10.60T \\ G^\circ(\text{UAl}_2) &= -22,790 - 2.326T \ln T + 18.37T \end{aligned}$$

where T is the temperature in degrees kelvin and the free energy is in cal/mole- °K.

The peritectic decomposition reaction for UAl_4 yielded 4.0 ± 0.4 kcal/mole at 1005°K.

SPECIFIC HEAT

Reactor calculations for the molar specific heat for aluminum-uranium alloys are determined using the ideal mixing equation. The molar specific heat is given by

$$C_p, \text{ U-Al} = (C_p, \text{ U} (235.04) (M\%) + C_p, \text{ Al} (26.98) (1.00-M\%)) / 100$$

where the specific heats for pure aluminum and uranium are shown in Figure 12.

2.5 Coefficient of Linear Expansion

When metals or alloys are heated, they expand according to the relationship $1 + \alpha \Delta T$ where α is the linear coefficient of expansion. The coefficient of linear expansion for 1100 aluminum and for 18 wt% U-Al alloy is shown in Figure 13. Also shown is the expansion coefficient for a 48 wt% U-Al alloy containing 3 wt% silicon⁶.

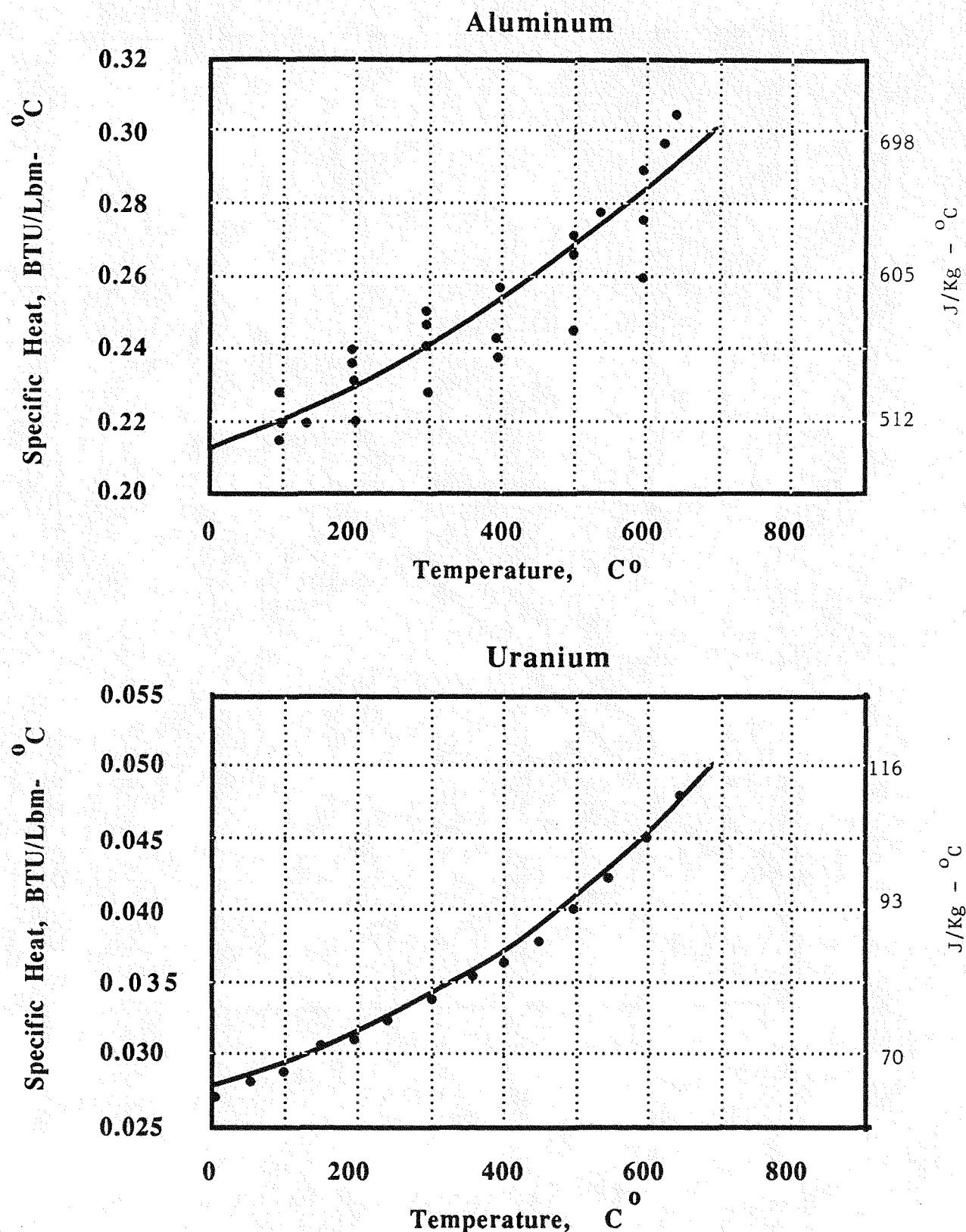


FIGURE 12. HEAT CAPACITY CORRELATIONS FOR ALUMINUM AND URANIUM

REFERENCE: Y. S. Touloukian, "Thermophysical Properties of Matter," Vol 1 & 4, IFI/Plenum, N.Y., 1970

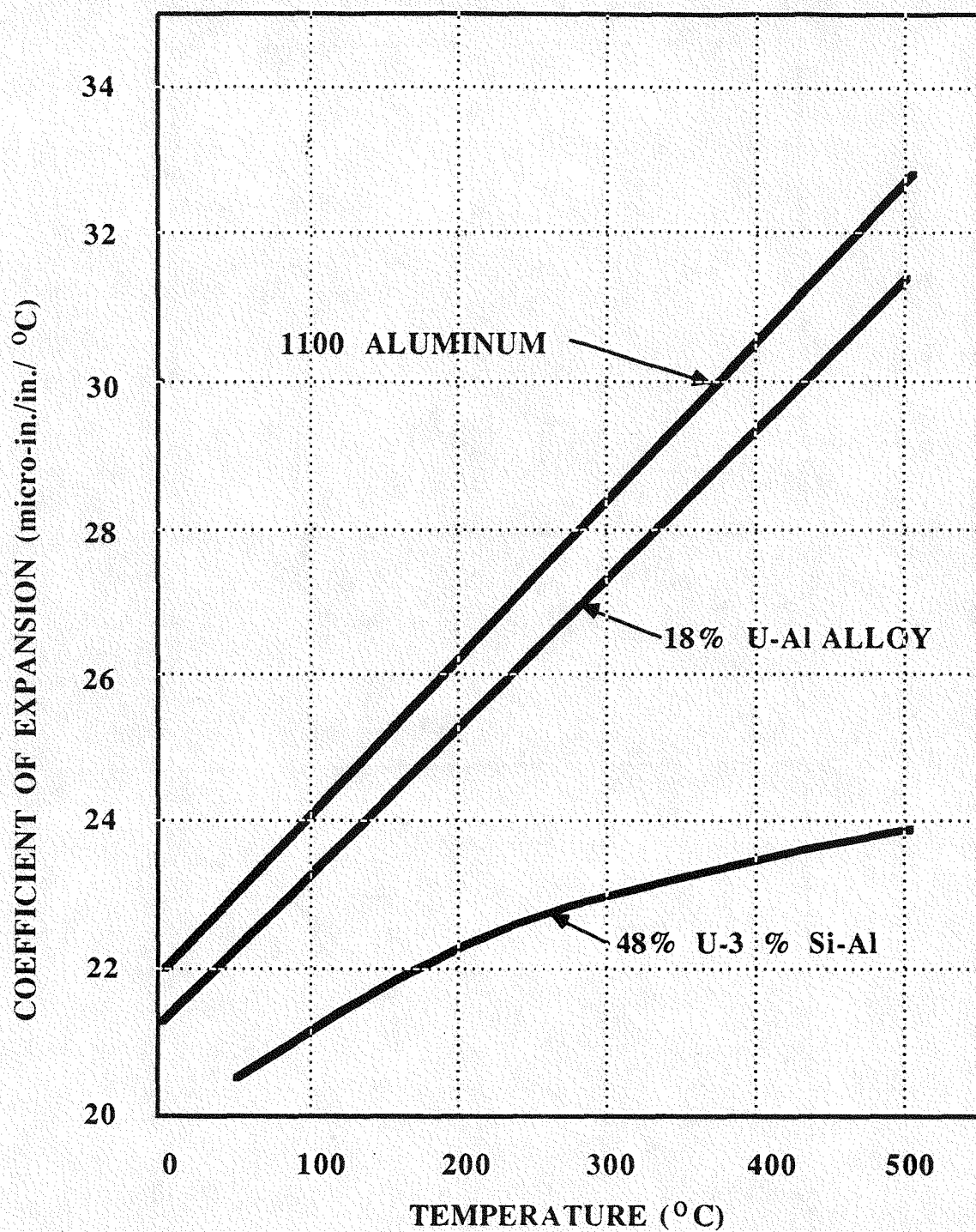


FIGURE 13. COEFFICIENT OF LINEAR THERMAL EXPANSION OF 1100 AI AND U-Al ALLOYS

REFERENCE: Thurber, W. C., and Beaver R. J., "Development of Silicon-Modified to Wt% U-Al Alloys for Aluminum Plate-Type Fuel Elements," ORNL-2602. 1955

For aluminum and the 18 wt% uranium alloy, the expansion coefficient is linear within the temperature range of 0 to 500°C. The expansion coefficients for aluminum and the 18 wt% alloy are close. Thermal stresses develop when two materials that have different expansion coefficients are bonded and heated.

The coefficient of linear expansion¹⁰ for different aluminum-uranium alloy compositions over several temperature ranges is given in Table IV. The data were obtained using 1/2-inch diameter specimens and standard dilatometric methods. For the 20-500 temperature range, there is an approximately 23% decrease in the average coefficient of expansion between pure aluminum and the aluminum -30.5 wt% uranium alloy. Heating and cooling curves were made from 50°C to 500°C. Data during heating and cooling were similar.

2.6 Mechanical Properties

Unirradiated Alloy

Mechanical properties at room temperature for unirradiated aluminum-uranium alloys containing 16 to 45 wt% uranium were determined by Gimpl and Huntoon¹⁶. Standard round or flat specimens with two-inch gauge lengths were used for all tensile tests. Data are shown in Table V.

Increasing the uranium content from 16 to 42 wt% in cast aluminum-uranium alloys, increased the hardness from 57 to 92 Rockwell "H". The yield strength increased from 8,400 psi to 12,000 psi, and the tensile strength increased from 13,000 psi to 19,600 psi. Elongation decreased from 4 to 1 %.

Hot working of cast alloys breaks up the large, friable UAl_4 particles and increased ductility, strength, and hardness for a given composition. Elongation of wrought alloys decreased rapidly from 17 to about 1.5% as the uranium content increased from 16 to 35 per cent uranium. From 35 to 43 per cent uranium, the elongation remained nearly constant at about 1.5%. The yield strength of these alloys increased from 12,300 psi at 16 wt% to 22,000 psi at 43 wt% uranium. Results are shown in Figure 14 for hot-rolled aluminum-uranium alloys. Cold working of hot worked alloys had little effect on the properties except to decrease ductility of alloys containing 25 and 35 wt% uranium.

Annealing, after cold working, increased the elongation of 30 and 35 wt% uranium alloys to 9.0 and 6.8%, respectively.

Saller¹⁰ obtained tensile properties of forged 12.5, 22.7 and 30.5 wt% uranium alloys which are tabulated in Table VI. These data were obtained using standard 0.505-inch tensile specimens machined from forged bars which had been annealed 1/2 hour at 370°C. Modulus determinations were made by first preloading the bars, then reloading and measuring the elongations with strain gages.

Elevated temperature tensile tests were also carried out at 150 and 300°C for aluminum-uranium alloys containing 11.3 and 17.3 wt% uranium. Results of these tests are given in Table VII and includes information on 2S aluminum. Properties of the two different uranium bearing alloys were about the same at corresponding elevated temperatures. Both were stronger but less ductile than pure aluminum at the same temperature.

TABLE IV
COEFFICIENT OF LINEAR EXPANSION
OF ALUMINUM-URANIUM ALLOYS

Average Coefficient of linear expansion, $10^{-6}/^{\circ}\text{C}$

Temp. Range, $^{\circ}\text{C}$	0 ^a Wt.% U Content	12.5 Wt.% U Content	22.7 Wt.% U Content	30.5 Wt.% U Content
20-100	23.9	20.0	20.0	19.4
20-200	24.6	21.1	21.2	20.8
20-300	25.5	22.1	21.9	21.3
20-400	26.5	23.1	22.5	21.6
20-500	27.7	23.5	22.7	22.1
100-500	-	24.4	23.2	22.6

^aMetals Handbook, 1948 edition (99.996% aluminum).

Reference: Saller, H. A. "Preparation, Properties and Cladding of Aluminum-Uranium, Alloys", Proceedings of the International Conference on the Peaceful Uses of Atomic Energy, Vol. 9, P/562, p214, United Nations, NY, 1956.

TABLE V
MECHANICAL PROPERTIES OF ALUMINUM-URANIUM ALLOYS

Condition	Composition, w/o U	LONGITUDINAL DIRECTION						TRANSVERSE DIRECTION					
		Tensile Strength, psi	Yield Strength (0.2% Offset), psi	Elongation in 2 in., %	Reduction in Area, %	Hardness, R _P	Hardness, R _H	Tensile Strength, psi	Yield Strength (0.2% offset), psi	Elongation in 2 in., %	Reduction in Area, %	Hardness, R _P	Hardness, R _H
As Cast	15.9	13,000	8,400	4.0	4.0		53-62						
As Cast	16.0	15,200	5,600	8.0	-		42-72						
As Cast	23.5	12,500	6,700	3.0	2.0		58-64						
As Cast	27.2	13,700	7,700	1.7	1.0		69-79						
As Cast	31.7	12,000	8,200	1.5	1.0		59-67						
As Cast	32.9	13,500	7,800	1.5	1.0		76-83						
As Cast	34.3	11,200	8,900	1.0	0.5		76-82						
As Cast	42.1	19,600	12,000	1.0	0.5		87-97						
Hot Rolled at 425°C	15.9	20,300	12,300	17.0	22.6	21	73	20,200	12,900	17.0	22.0	25	77
Hot Rolled at 565°C	16.0	16,600	6,100	25.0	-								
Hot Rolled at 565°C	26.1	20,700	17,100	7.0	15.4	36	82						
Hot Rolled at 565°C	27.5							19,600	16,000	6.0	8.5	43	86
Hot Rolled at 565°C	28.1							22,200	17,800	6.1	6.9	44	88
Hot Rolled at 565°C	30.0	21,600	18,000	6.1	8.3	45	86						
Hot Rolled at 565°C	35.0	22,600	21,500	1.5	2.7	48	89	21,800	20,200	1.0	1.2	48	90
Hot Rolled at 565°C	35.2	23,400	20,900	1.5	2.7	48	90	23,400	20,300	1.8	2.4	50	91
Hot Rolled at 565°C	43.2	26,000	22,100	1.0	1.4	67	97	22,900	22,500	0	67	67	98
Cold Worked 6.3%	26.5	22,300	20,900	2.5	4.4	44	88						
Cold Worked 10.0%	27.3							21,100	19,100	3.0	3.8	40	87
Cold Worked 10.0%	30.0	23,500	21,400	3	3.6	48	88						
Cold Worked 6.3%	35.0	23,100	20,200	1.5	2.6	45	89	22,200	20,200	1.5	3.0	44	89
Cold Worked 6.3%	35.2	22,600	18,800	2	4.1	46	89	22,600	20,000	1.5	2.8	47	90
Cold Worked 20%	23.8	22,700	20,100	2	4.5	44	87						
Cold Worked 20%	28.1							23,200	20,500	1.5	3.0	46	87
Cold Worked 20%	30.0	23,500	21,500	1.5	2.8	49	91						
Cold Worked 17%	35.0	22,900	20,000	1.5	1.3	48	90	22,300	20,600	0.8	2.1	47	90
Cold Worked 17%	35.2	23,000	20,700	1.5	2.3	48	90	23,300	20,600	1.5	1.3	49	91
Cold Worked 20%	30.0	18,600	10,500	9.0	8.5								
Annealed at 540°C for 2 hr													
Cold Worked 20% Annealed at 540°C for 2 hr	35.0	16,800	10,100	6.8	6.7								

Reference: Gimple, M. L. and Huntoon, R. T., "Properties of Aluminum-Uranium Alloys Containing 16 to 45 Percent Uranium," E. I. du Pont de Nemours & Co., DP-256, 1957

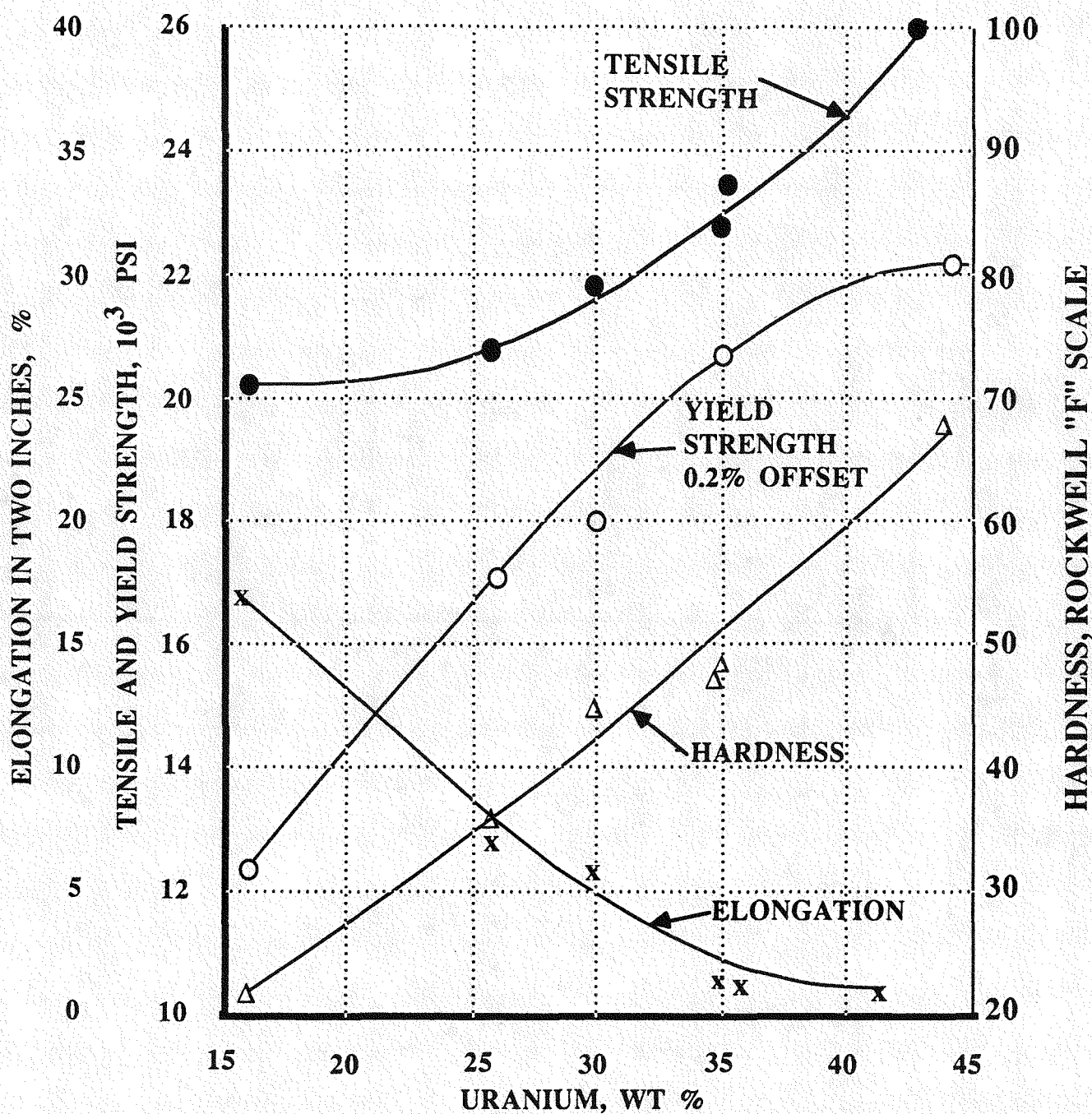


FIGURE 14. EFFECT OF COMPOSITION ON THE MECHANICAL PROPERTIES OF HOT-ROLLED ALUMINUM-URANIUM ALLOYS

REFERENCE: Gimple, M. L., and Huntoon, R. T., "Properties of Aluminum-Uranium Alloys Containing 16 to 45 Percent Uranium," E.I. du Pont de Nemours & Co., DP-256, 1957

TABLE VI
TENSILE PROPERTIES OF FORGED ALUMINUM-URANIUM ALLOYS

Composition, wt. % U	Average modulus of elasticity, a 10^6 psi	Tensile strength, psi	Yield strength (0.2% offset), psi	Elongation, %	Reduction in area, %
0 ^a	10.0	13,000	5,000	45	
12.5 ^b	10.4	22,500	10,800	20	34
22.7	10.9	18,600	11,600	4	7
22.7	11.3	23,500	14,500	13	14
30.5 ^b	11.3	26,100	14,850	10.5	11.5

a Estimated to be correct within +3%.

b Single specimens were used.

Reference: Saller, H. A. "Preparation, Properties and Cladding of Aluminum-Uranium, Alloys", Proceedings of the International Conference on the Peaceful Uses of Atomic Energy, Vol. 9, P/562, p214, United Nations, NY, 1956.

TABLE VII
HIGH-TEMPERATURE PROPERTIES* OF ALUMINUM-URANIUM ALLOYS

Alloy	Room Temperature			150°C			300°C		Reduction in area, %
	Tensile Strength, psi	0.2% Offset Yield Strength, psi	Elongation, %	Tensile Strength, psi	0.2% Offset Yield Strength, psi	Elongation, %	Tensile Strength, psi	Elongation, %	
2SO aluminum	13,000	5000	45+	7500	3500	65	2500	90	-
11.3 weight % uranium	19,700	11,320	28	14,125	9200	31	8630	31	57
17.3 weight % uranium	20,080	11,480	28	14,700	10,000	27	8780	34	60
	19,030	8550	30	14,000	7230	34	8130	48	59.5
				13,650	7020	35	8210	42	58
				13,300	6480	35	-	-	-

* Tests on metal annealed at 370°C for 1 hour; 2SO values from "Alcoa Aluminum and Its Alloys".

+ Elongation in 2 inches, others in 1 inch.

Reference: Saller, H. A., Preparation, Properties, and Cladding of Aluminum-Uranium Alloys, in Proceedings of the International Conference on the Peaceful Uses of Atomic Energy, V9, p/562, P214, United Nations, New York, 1956.

Irradiated Alloy

Gibson¹⁷ et al. completed microhardness tests on several irradiated aluminum-uranium alloy fuel samples. The results indicated a general increase in hardness with irradiation. The hardness of the U-Al alloy matrix showed greater increases than the aluminum cladding.

Tensile tests were also done on 94 different irradiated fuel plates containing either aluminum-uranium, UO_2 -aluminum, or U_3O_8 -aluminum dispersion fuel¹⁷. The major change in mechanical properties from fission damage was a loss in ductility. At irradiation levels of about 2×10^{20} neutrons/cm², thermal, the maximum elongation for any one specimen was 4.5%. At 2×10^{21} the maximum was only 1% while at 2.6×10^{21} it was zero. In all ranges of exposure, some of the specimens showed zero ductility. Two specimens broke in three pieces but many separated at the core/clad interface. Tensile strength of the material increased from 3 to 125% with most increases falling between 30 and 80%. Two tests showed a decrease in tensile strength.

3.0 CHEMICAL PROPERTIES

3.1 Aluminum Fuel Water Reactions

Cast and wrought aluminum-uranium alloys with up to 15 wt% uranium were corrosion tested in an autoclave at temperatures of 350 °C¹⁸. High weight percent uranium alloys exhibited intergranular attack at exposed ends of the samples. From the test results the following conclusions were made:

- (1) Aluminum alloys containing less than 6 weight percent uranium are not satisfactory high temperature fuel element cores from the standpoint of swelling in case of jacket failure.
- (2) Al-Si alloys containing up to 6 weight percent uranium are satisfactory. Higher uranium contents are probably also satisfactory but were not tested.
- (3) As-cast aluminum alloys containing 6-15 weight percent uranium are comparable to Al-Si and are preferable to Al-Si because of the separations problem presented by silicon.

Rutherford and Draley¹⁹ carried out sixty day corrosion tests in water at 290°C. The samples were unirradiated aluminum-uranium alloys containing 2 wt% nickel and 1/2 wt% iron. The uranium contents ranged from 15 to 53 wt%. The maximum metal penetration rate was found to be 14 mils per year by extrapolation. This rate is about twice the penetration rate for X8001 aluminum cladding alloy at the same temperature.

Corrosion rate for 15 wt% alloy was 9.4 mg/dm²/day (mdd) while the corrosion rate for a 53 wt% alloy was 5.3 mdd. A sharp transition in corrosion behavior occurred at UAl_2 composition.

Corrosion resistance of aluminum-uranium alloys containing up to 45 wt% uranium in water was also studied by Daniel et al.²⁰ The resistance exhibited by higher uranium content alloys was comparable to the aluminum-16 wt% uranium alloy. The diffusion of uranium from the alloys into 2S aluminum after 30 days at 750°F could not be detected by metallographic techniques.

3.2 Irradiated Fuel-Water Reactions

A TREAT (Transient Reactor Test facility) experiment was carried out using preirradiated samples of an aluminum- 17 wt% uranium alloy fuel plate to determine the effect of preirradiation on the extent of the metal-water reaction²¹. The fuel was preirradiated to a 2.2% burnup of the heavy atoms. It was concluded that preirradiation did not influence the extent of the fuel-water reaction.

3.3 Fuel Steam Reactions

Studies of isothermal reaction of aluminum-17 wt% uranium alloy with steam were carried out over the temperature range of 1200°C to 1600°C.^{22,23} The results showed that the reaction could be described by the same cubic rate law used to express the reaction with steam below 1300°C and expressed in the earlier report.

An extensive review of the literature has been done recently regarding particle size distribution, particle surface area, oxidation rate, and pressure generation of aluminum clad, aluminum-uranium fuel during a core meltdown²⁴. The primary concerns listed were: (a) confinement failure from hydrogen deflagration or detonation; (b) metal-water steam explosion; and (c) recriticality after fuel relocation.

Previously unpublished data from Morin²⁵ was cited in this report which indicated that the reaction with high velocity steam produced intergranular melting with extensive fragmentation.

Experiments on the reaction of molten SRP reactor fuel with water were reviewed by Morin and Hyder at an ANS Workshop at Idaho Falls, Idaho²⁶. The reaction was described as extremely complex, even chaotic. At temperatures approaching the melting point of aluminum, the reaction rate is quite low because aluminum oxide on the surface impedes reactions with aluminum. When aluminum melts, mixing occurs so that steam explosions result. Chemical reactions can occur during the course of an explosion. Long term exposure produces gaseous fission products which may cause foaming of the fuel material as it melts. Also, transmutation of aluminum into silicon may decrease the melting point of aluminum alloys. Experiments are continuing to better define these areas of concern.

4.0 IRRADIATION PERFORMANCE

4.1 Irradiation Conditions

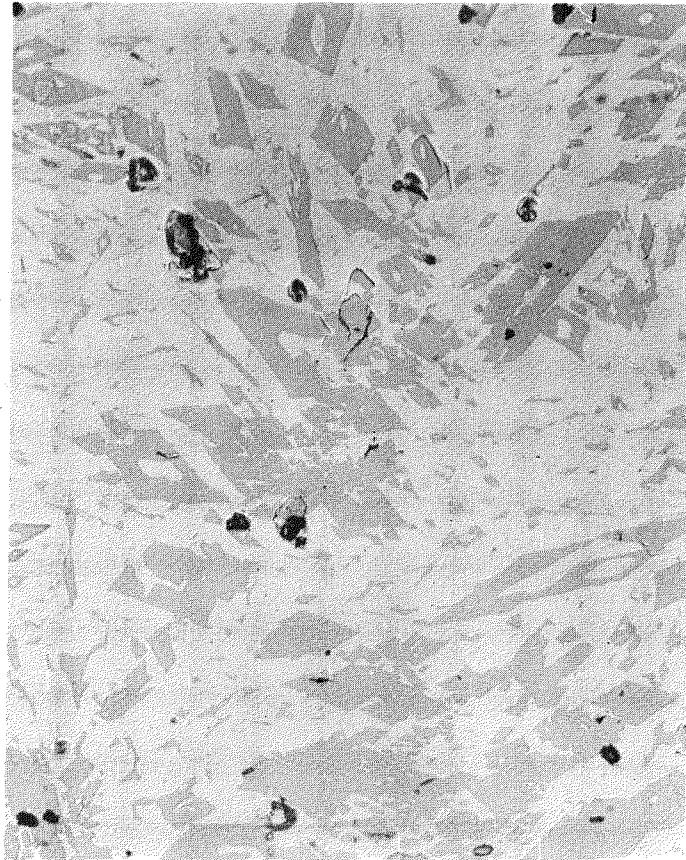
Kittel, Gavin, Corthers and Carlander²⁷ described irradiation experiments to determine temperature and burnup limits for Aluminum-17.5 wt% uranium containing 2 wt% Ni and 0.5 wt% iron and clad with X8001 aluminum. Irradiations were conducted in the MTR. One of the plates developed a cladding defect in high pH water. At the time the defect developed, the plate had a burnup of 58 percent of the uranium. No catastrophic corrosion of the fuel alloy or extensive fission product release occurred when the plate was irradiated with the defect. Conclusions reached were:

- 1) Aluminum alloy-clad aluminum-uranium alloy fuel plates of the SL-1 type are capable of operation to burnups on the order of 50 percent of the uranium (1 percent total atom burnup) at fuel temperatures exceeding 400°C.
- 2) Cladding failure of aluminum alloy-clad aluminum-uranium alloy fuel plates is more apt to result from penetration by pitting corrosion than from fuel swelling.
- 3) Aluminum-uranium alloy plates clad with X8001 aluminum alloy can be operated successfully under local boiling conditions in neutral water at 215°C.
- 4) Exposure of defected highly-irradiated Aluminum-17.5 wt% uranium fuel alloy to water at 215°C does not result in catastrophic corrosion or cause the release of large amounts of fission product activity.

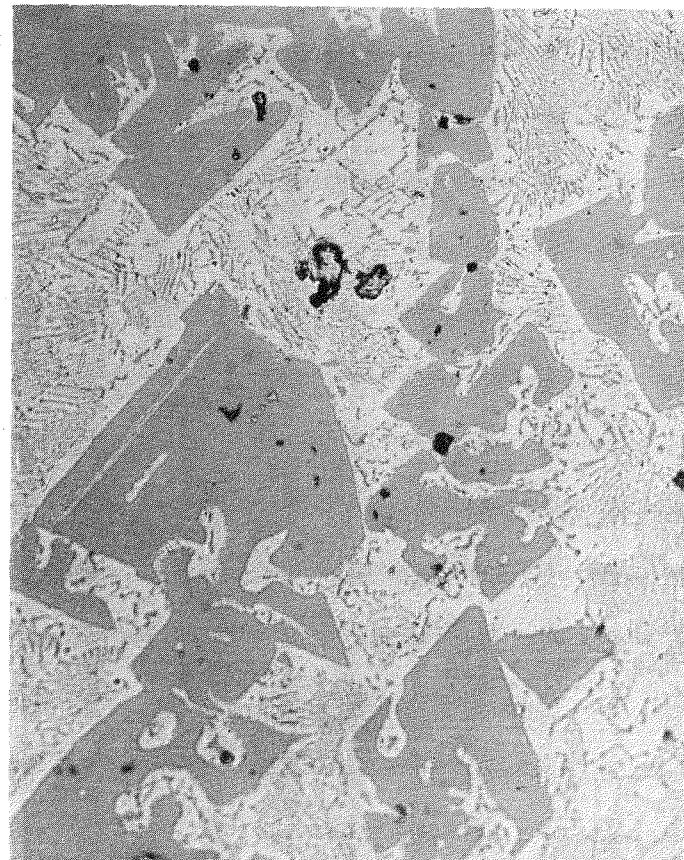
4.2 Microstructure

Microstructures of cast, unirradiated aluminum-uranium alloys are shown in Figure 15 for two different uranium contents. The primary aluminides change shape from an acicular type structure for UAl_4 to a "blocky" type structure for UAl_3 . UAl_4 particles in unirradiated alloys usually contain cracks which are formed during metal working operations.

Caskey and Angerman^{28,29} studied the microstructure of irradiated aluminum-uranium fuel using replicated samples. The alloy in a Mark VIJ fuel tube containing 1430g of ^{235}U was irradiated to an average burnup of 494 MWD. No cracks were observed in irradiated UAl_4 particles which was probably due to sintering of the uranium containing particles during irradiation. Gas bubbles were observed along aluminum/ UAl_4 boundaries and some were observed in UAl_4 particles. The bubbles were found particularly in matrix areas bounded on three sides by the UAl_4 intermetallic compound. It was hypothesized that the gas in the matrix resulted from fission recoil and diffusion from the UAl_4 particles. Photomicrographs of as-irradiated material are shown in Figures 16 and 17a.



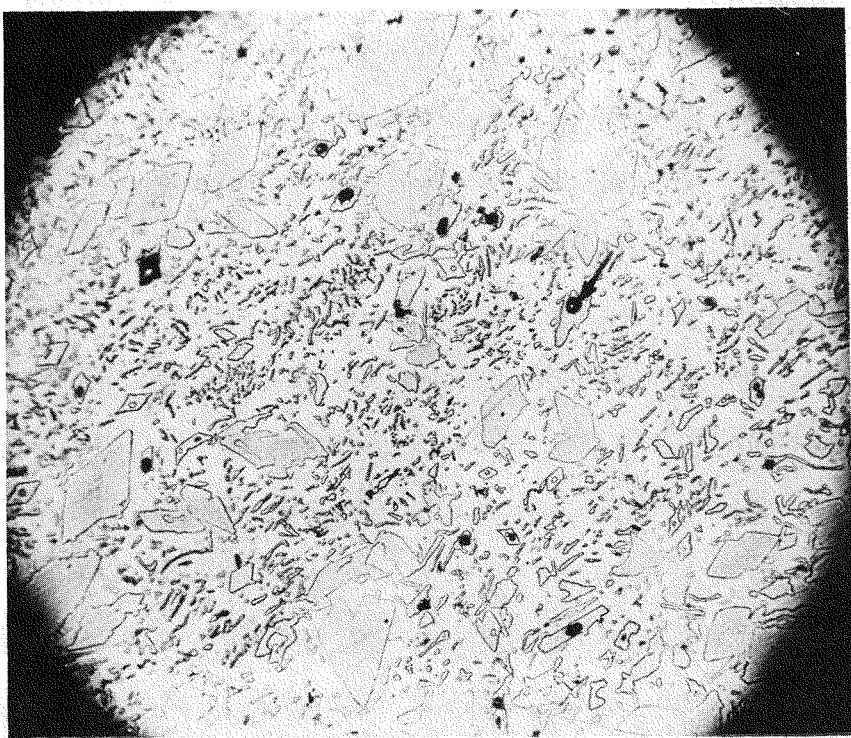
a) UAl₄



b) UAl₃

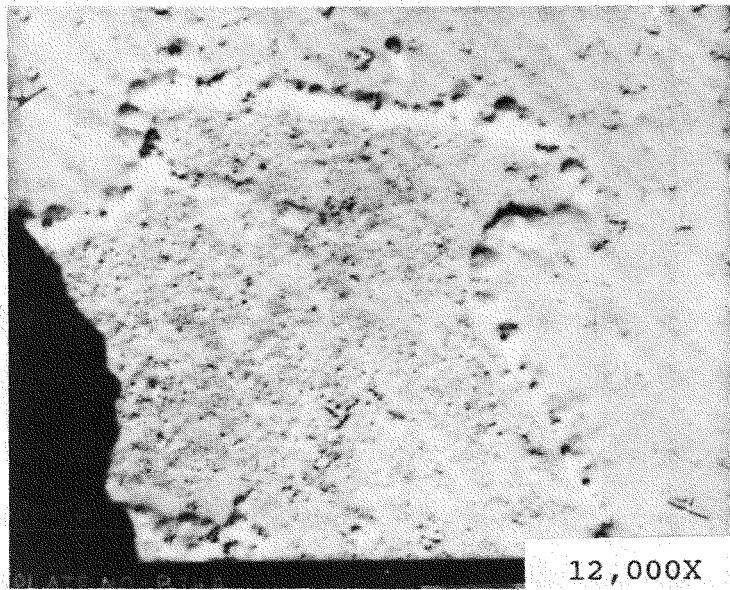
.005"

FIGURE 15. MICROSTRUCTURE OF CAST ALUMINUM-URANIUM ALLOYS SHOWING UAl₄ and UAl₃ PRIMARY PHASES

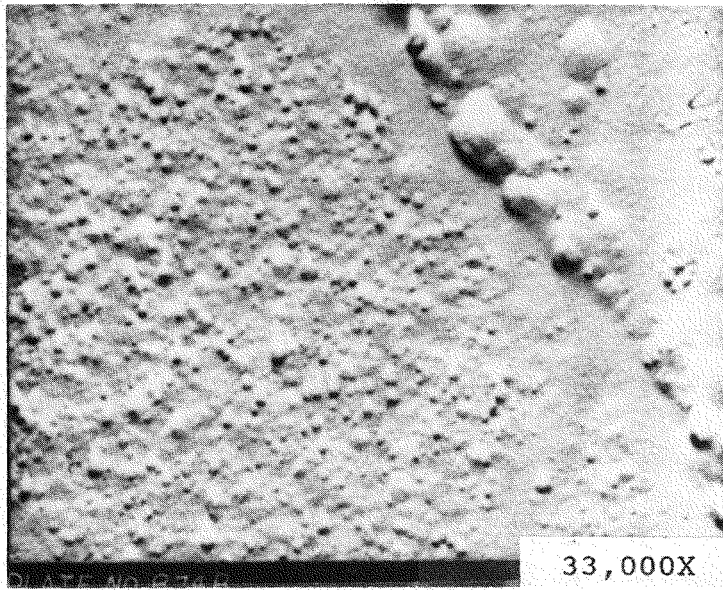


a) Optical Photomicrograph

Numerous holes observed within UAl₄ particles which were probably due to sintering of cracked particles. As-Irradiated. 250x



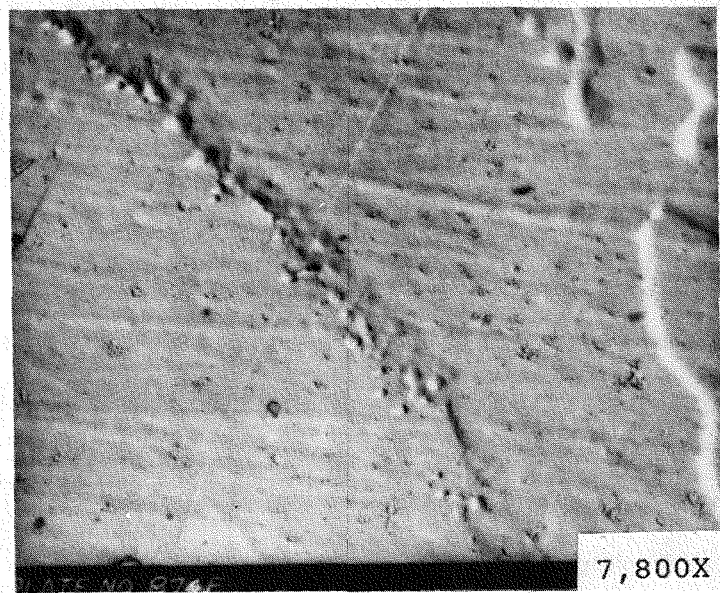
12,000X



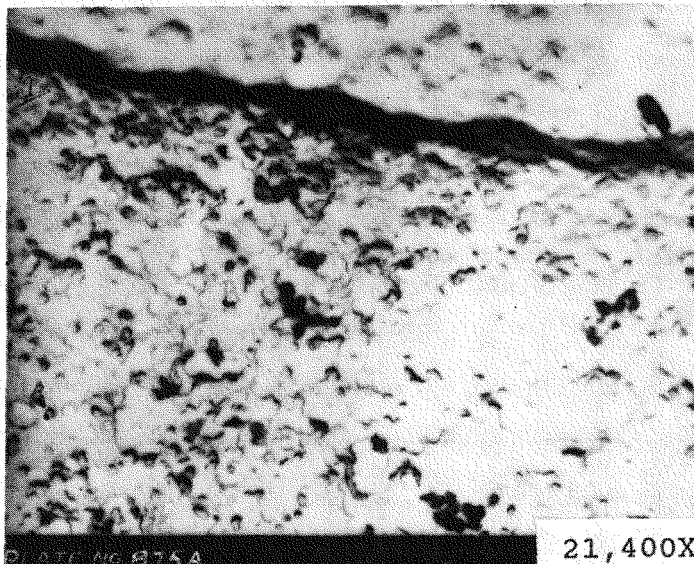
33,000X

b) Fission gas bubbles observed along the Aluminum/UAl₄ boundaries and a mottled appearance within the aluminum matrix which appears to be holes, probably from fission gases. As Irradiated.

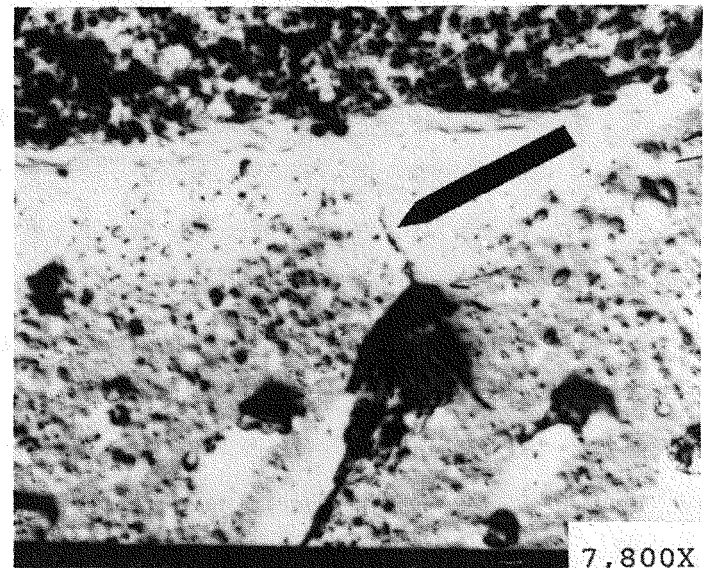
FIGURE 16. PHOTOMICROGRAPHS OF IRRADIATED ALUMINUM-URANIUM ALLOYS



a) Fission Gas Bubbles at the Interface Between Two UAl₄ particles in As-Irradiated Aluminum-Uranium Alloy. 7800x



b) Irradiated Alloy Heated 48 hours at 400°C. Fission gas bubbles found in UAl₄ particles. 21,400x



c) Irradiated Alloy heated at 550°C. Cracks were observed extending from UAl₄ particles. 7800x

FIGURE 17. IRRADIATED AND ANNEALED ALUMINUM - URANIUM ALLOYS

Irradiated samples were annealed and microstructural changes were recorded. Based on these changes, it was postulated that increased annealing temperatures caused the aluminum-uranium alloy to swell because of increased nucleation and growth of gas bubbles both within the UAl_4 particles and in the matrix near the particles as shown in Figure 17b. At 550°C, cracking occurred as shown in Figure 17c. Cracks started at UAl_4 particles and propagated into the aluminum matrix. No cracking of the UAl_4 particles was observed.

Hofman³⁰ carried out SEM examinations of irradiated UAl_x -aluminum dispersion fuel. Evidence suggested that UAl_2 , UAl_3 and UAl_4 do not form fission gas bubbles at fission densities of $7 \times 10^{21}/cc$ of fuel and that pure uranium-aluminide is likely to remain free of fission gas bubbles to very high burnups. However, fission gas bubbles within UAl_x particles were associated with uranium-oxide inclusions.

Fission gas diffusion in 20 wt% uranium-aluminum was reported³¹. The three basic diffusion steps for fission gas movement are:

- 1) diffusion of gas from within the fuel particle to the phase boundary between the particle and matrix.
- 2) solution of the gas in the matrix
- 3) diffusion of the gas through the matrix to a free surface from which it can escape.

Results showed that there was excellent gas retention by UAl_4 particles in a low burnup alloy at temperatures below the melting point of the matrix. When the matrix melted, a large amount of fission gas was released. Since rare gases are insoluble in metals, then it appeared that the particle-matrix boundary was an effective barrier for escaping fission gases.

4.3 Swelling and Blister Threshold Temperature of Al-U Alloys

A characteristic common to all fuel elements is dimensional stability during irradiation. Stability can be expressed as general swelling of the fuel element with irradiation time or blistering which is the formation of large blisters on the surface.

SWELLING

During irradiation fission gases or microstructural changes occur which can effect uniform swelling of fuel elements. There is generally an increase in fuel diameter and/or wall thickness as a function of irradiation time. Void content associated with porosity and fabrication can effect swelling of fuels as well as volume changes occurring from reactions. Voids are low energy sites for possible accumulation of fission gases and thus can influence swelling behavior.

Postirradiation annealing tests to define dimensional stability of irradiated 17.5 wt% aluminum-uranium alloy were done at Argonne National Laboratory³². Studies used coupons cut from irradiated fuel plates. The annealing studies were carried out in a salt bath. At a burnup of 1.6×10^{20} fissions/cc, the alloy had excellent resistance to swelling up to 550°C. At burnups of 5.5×10^{20} fissions/cc, swelling occurred at 550°C.

Extruded fuel tubes swelled during irradiation at Savannah River from fission gas bubbles that were located primarily in the aluminum matrix of the core²⁹. Tubes had been irradiated to approximately 43% burnup. Analysis of tube sections indicated the fuel temperature was probably higher than 400°C. Annealing tests were done on postirradiated fuel sections. Tests showed the formation of fission gas bubbles and then cracks in the fuel sections. At 550°C extensive cracking occurred, resulting in a 25% volume increase.

Swelling of irradiated aluminum-25 wt% uranium alloy was evaluated by Caskey and Angerman^{28,33}. Specimens annealed at 400°C swelled very little, 0.3%. Swelling, which was caused by the formation of fission gas bubbles in the aluminum matrix, ceased after 25 hours of heating at 400°C. No further swelling occurred for annealing times up to 100 hours, and no cracks were visible. Specimens annealed at 475° and 550°C cracked extensively. These cracks accounted for essentially all of the measured volume increase and frequently followed the grain boundaries of the aluminum matrix.

Swelling was determined from density measurements. The volume increase is shown in Figure 18 as a function of annealing time. At 400°C, a small increase in volume was observed during the first 25 hours of heating while further heating did not cause additional changes. At 475° and 550°C, the logarithms of the volume (density) change vs log-time are linear functions.

The volume of cracks in the specimens were determined metallographically. The data, shown in Figure 19, indicate a steadily increase crack volume with increases in time and temperature above 400°C. The rate of crack-volume-increase decreases with heating time.

A 30 wt% aluminum-uranium alloy fuel element, clad with 8001 aluminum, was irradiated in HFBR test reactor and was examined in MTR hot cells³⁴. The plates warped and bowed but little swelling and no blistering was observed. Bend tests showed fracture after a 15° bend on a 1-inch radius. Punchings for metallographic examination were extremely brittle and showed brittle failure of the cladding.

BLISTERING

Fuels exhibit a temperature at which large localized volume increases occur in a short time. Blisters form from increased gas pressure in the core. This temperature is called the Blister Temperature. Operation of fuel elements above the blister temperature is not practicable.

Fuel plates with 17.5 wt% uranium in aluminum and clad with M388 aluminum (2S aluminum with 1% nickel) were irradiated in MTR³⁵ and were examined in the hot cells. The loop water temperature was 420°F and the heat flux of 690,000 initially and 260,000 BTU/hr·ft² at the end of cycle. Irradiation was discontinued after a maximum burnup of 58% of the original 2.2 atom per cent of total ²³⁵U.

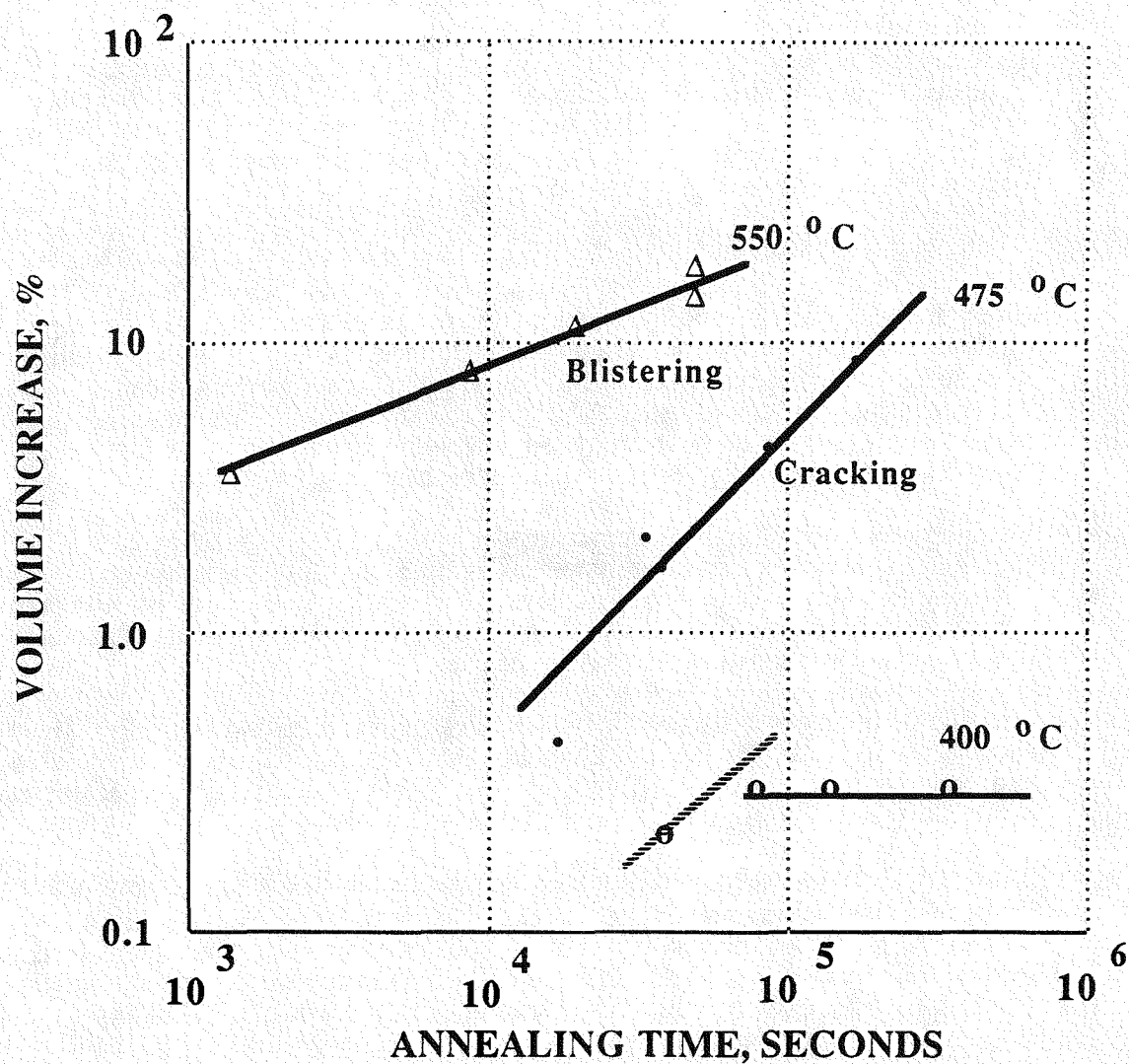


FIGURE 18. SWELLING OF IRRADIATED Al-U (25 wt.%) ALLOY DURING ANNEALING

REFERENCE: Caskey, G.R., and Angerman, C.L., "Swelling of Irradiated Aluminum-Uranium Alloy During Post Irradiation Annealing," E. I. du Pont de Nemours & Co., DPST-65-351, 1965.

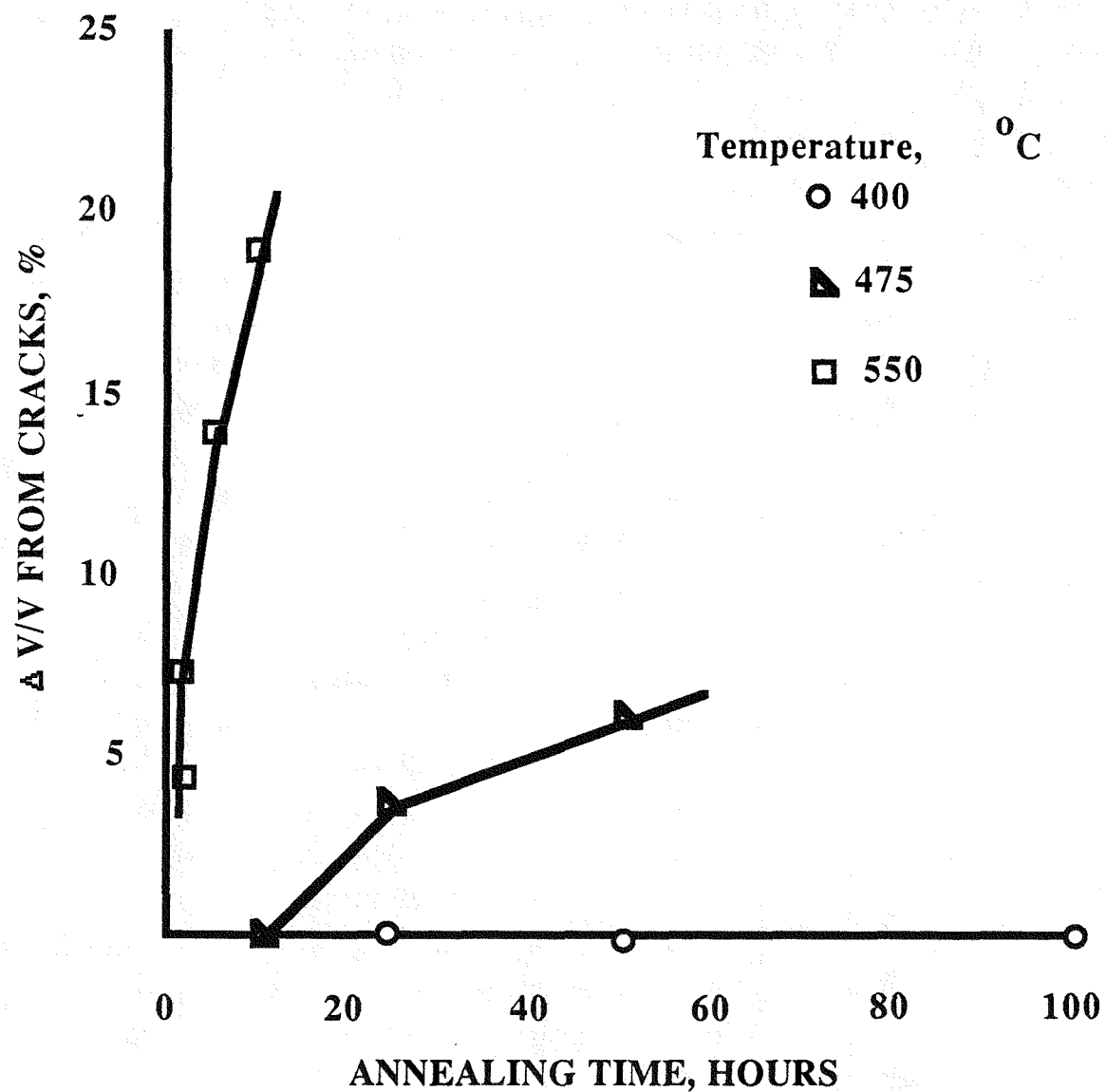


FIGURE 19. VOLUME INCREASE DUE TO CRACKS FORMED DURING ANNEALING OF IRRADIATED Al-25 WT% U ALLOY

REFERENCE: Caskey, G. R. and Angerman, C. L., "Swelling of Irradiated Al-U Alloy During Post Irradiation Annealing," E. I. du Pont de Nemours & Co., DPST-65-351, 1965

Post irradiation examination showed two blisters which were filled with corrosion products. Swelling was observed also at the highest neutron flux and was attributed to a combination of high burnup and high fuel temperature. It was estimated the fuel reached 1000°F (538°C) as a result of high burnup and a thick oxide layer.

For an extruded aluminum -25wt% uranium alloy, several large blisters occurred after 5 hours at 550°C.³³ Extensive cracking of the core occurred above 400°C which would eventually lead to gross blister formation.

5.0 IN-REACTOR FUEL BEHAVIOR

Uranium-aluminum alloy fuel has been irradiated successfully in SRS production reactors as well as in many international research and test reactors. Failure of alloy elements has occurred during routine irradiations but no known melt-down or severe accident has taken place. The behavior of alloy fuel in this report is based on SRS experience of element failures and severe accident test results obtained from tests in TREAT³⁶ AND SPERT I³⁷.

5.1 Fuel Element Failures

SRS EXPERIENCE

The Savannah River Site (SRS) has irradiated fuel assemblies with cast aluminum-uranium cores since about the 60's. The approximate number of tubes irradiated in SRS reactors is over 200,000. The uranium content of the cores has increased over the years to the present concentration of 33 wt% uranium in aluminum. Tube geometry has included Mark 14, Mark 16 and Mark 22 type drivers shown schematically in Appendix 1.

The irradiation performance of cast aluminum-uranium alloys has been good. Fuel failures recorded since 1969 are 10 Mark 18 tubes in 1969-70 which had some melting near the bottom 2 feet of the outer tubes³⁸ and 42 Mark 22 tubes containing cladding penetrations in 1971-72³⁹. Penetrations resulted wherever the residual cladding thickness over agglomerates of uranium aluminide particles was less than that consumed by normal in-reactor corrosion⁴⁰. Since about 1972, all fuel tubes have been fluoroscopically inspected as part of the manufacturing area's quality control program. No indication of tube failures was found until 1982 when 3 Mark 22 reactor failures were suspected.

Fuel assemblies have operated at power levels up to about 7 megawatts(MW). With the exception of increased moderator activity from above failures, no other problems have been recorded with the use of cast aluminum-uranium alloy fuel in SRS reactors.

5.2 Severe Accident

Reactor accident analysis studies and tests are the subject of research at several Laboratory sites. A recent report⁴¹ provides a review of the issues related to bounding thermodynamic calculations.

Calculations were made for several consequences contributing to containment pressurization during severe accidents such as a loss-of-coolant and loss-of-pumping accidents. The results are shown in Table VIII, with material physical properties used in these calculations shown in Table IX. Peak containment pressures varied from <2 psig for blowdown to 80 psig for total cooling failure.

TABLE VIII
WORST CASE CONSEQUENCES ATTENDING
PRESUMED COOLING SYSTEM FAILURES

Consequences	Failed Systems*	Peak Containment Pressures (psig)
Blowdown	PCS	<2
Steam Explosion	PSC BRHRS, ECCS	
Metal Heated by Decay†		8 (Unfocused)
Re-criticality†		10 (Unfocused)
Containment Heating, Adiabatic	PCS, BRHRS, ECCS, CHRS Sprays	20 (At 0.75 hr)
Direct Containment Heating Event from Dry Re-criticality	PCS, BRHRS, ECCS, CHRS Sprays	28 (At 0.75 hr)
Total Cooling Failure	PCS, BRHRS, ECCS, CHRS Sprays, CHRS Fan Coolers	80 (At 0.75 hr) (See Note 1)
Core-Concrete Reaction and Hydrogen Explosion		0 (See Note 2)

Notes

* Systems

PCS - Primary Coolant System
 BRHRS - Backup Residual Heat Removal System
 ECCS - Emergency Core Cooling System
 CHRS - Containment Heat Removal System.

1. Not a peak pressure: it is presented to show that containment failure is expected under conditions with no cooling at all.
2. Considered impossible because of engineered safeguards (hydrogen igniters, water-free ceramics underneath reactor).

† Includes metal-water reaction

Reference: Hyder, M. L. and Parks, P. B., "Severe Accident Analysis for the NPP-HWR: Bounding Thermodynamic Calculations," E. I. du Pont de Nemours & Co., DPST-88-383, April 1988.

TABLE IX
QUANTITIES USED IN HEAT CALCULATIONS

Aluminum

Weight

- fuel and cladding, 18.9 metric tons (MT).
- fuel endfittings, 4.5 MT
- targets, 12.3 MT.
- housing tubes, 5.7 MT.

Heat Capacity, 0.215 cal/g °K.

Heat of Fusion, 94 cal/g.

Uranium

Weight (in fuel cores), 3.72 MT.

Heat Capacity, 0.0271 cal/g °K.

Heat of Fusion, 12.5 cal/g (not used in calculations).

Stainless Steel (calculated as iron)

Weight

- reactor lower vessel, 158 MT
(76 MT in Shield Rashig rings).
- reactor upper vessel, 169 MT
(90 MT in Shield Rashig rings).

Heat Capacity, 0.11 cal/g °K.

Air

Weight, 53.5 MT.

Volume, 56,400 m³, originally at 373°K.

Heat Capacity, 0.186 cal/g °K.

Total Heat Capacity of the System 5.50×10^7 cal/°K or 230 MJ/°K.

Reference: Hyder, M. L. and Parks, P. B., "Severe Accident Analysis for the NPR-HWR: Bounding Thermodynamic Calculations," E. I. du Pont de Nemours & Co., DPST-88-383, April 1988.

Small samples of aluminum-enriched-uranium alloy plates were subjected to nuclear transients in TREAT to determine the extent of metal/water reactions during an irradiation transient. The uranium contents of the plates were 23 wt% and 77 wt% uranium. Both clad and unclad specimens were tested. The samples were placed in an autoclave with distilled water and subjected to energies of 174 to 1023 cal/g of plate for periods of 42 to 112 msec. Heating of the fuel specimens from 25°C to 2480°C was obtained in less than 0.4 sec.

The extent of reaction with water for clad and unclad plates is shown in Figure 20. There were three regions of reaction which were a function of energy input.

- 1) In the first region, the extent of reaction increased for both types from negligible amounts (<0.1 percent) at an energy input of 174 cal/g to 7.2 percent at 530 cal/g.
- 2) At energies higher than 530 cal/g, the extent of reaction increased for both material types. The unclad plates reacted to a greater extent than clad plates in the second region with as much as 22.2 percent of an unclad plate having reacted at 740 cal/g. The differences in extent of reaction were explained as cladding and geometry differences.
- 3) Above 704 cal/g, a third region of very extensive reaction (> 35 percent) was observed.

The threshold for particle breakup was found to occur at energy inputs of 361 and 430 cal/g. The average surface-to-volume diameter of the particles in the most energetic transient with the clad plate was 0.0186 in. Above 256 cal/g no pure cladding material could be found.

Fuel meltdown experiments were reported by Seaboch and Wade for 31 wt% uranium-aluminum alloy fuel that was clad with 0.03 inch of aluminum. The test was conducted in the SPERT I reactor. The tubes melted to various degrees of severity. Molten fuel flowed down the sides of the fuel tubes, and some material was dispersed into the coolant and carried out in molten form with the effluent.

The heat flux encountered during the tests ranged from 200,000 to 650,000 $\frac{\text{BTU}}{\text{ft}^2 \text{ m}}$.

The time required for the metal temperature to reach the melting point from the time when burnout began varied from 1.3 to 4.9 seconds. Pressure pulses were produced at a frequency of about one per second with peaks of about 150 psi.

From the most severe meltdown, about 7% of the mass of the fuel tube was recovered as particles, which varied in size from tiny flakes to a jagged agglomerate weighing 37 grams. The temperature of the aluminum housing tube that surrounded the fuel tube did not exceed about 170°C, and the temperature of the aluminum tube that contained the fuel housing did not greatly exceed the ambient temperature. No chemical reactions occurred, and no detectable amount of uranium remained suspended in the water after the tests.

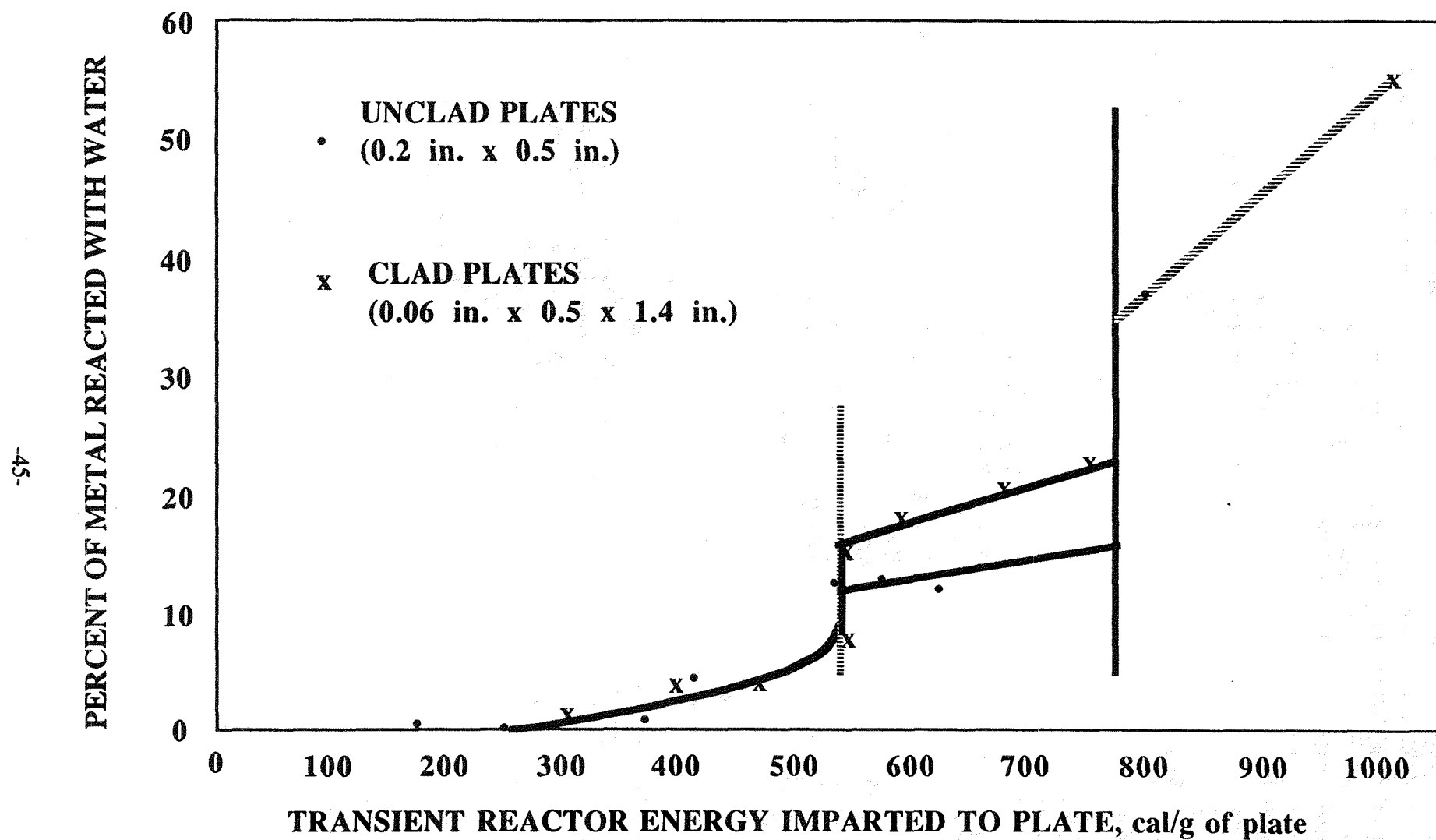


FIGURE 20. EXTENT OF REACTION OF U/Al PLATES WITH WATER RESULTING FROM DESTRUCTIVE TRANSIENT IRRADIATIONS

REFERENCE: Ivins, R. O., "A Study of the Reaction of Aluminum/Uranium Alloy Fuel Plates with Water Initiated by a Destructive Reactor Transient," Trans. Am. Nucl. Soc., 6;, pp 101-2,19.

6.0 FISSION PRODUCT RELEASE

6.1 Gases and Volatiles

Fission product release studies using irradiated UAlx-aluminum dispersion and aluminum-uranium alloy fuel elements have been done by several investigators. The release of fission gases from irradiated dispersion fuel is expected to be similar to the release from cast alloy fuel. Both fuels contain UAlx particles in essentially an aluminum matrix.

UAlx-ALUMINUM DISPERSION FUEL

UAl Alloy

Fission product measurements on UAlx miniplates were performed at Oak Ridge⁴². Irradiated uranium-aluminide plates with 40% ^{235}U enrichment were heated to determine the amount of fission products released at temperatures up to and higher than the melting point of the fuel cladding material. The release of fission products from the fuel plate at temperatures below 500°C was negligible. Three stages of fission product release were observed. The first rapid release was observed at about 561°C along with blistering of the plates. The next release, which occurred at 585°C, might have been caused by melting of the Type 6061 aluminum alloy cladding. The sum of these two releases accounted for about 70% of the total amount of fission products produced. The last release of fission product gases occurred at 650°C, which corresponds to the eutectic temperature of the uranium-aluminum alloy.

The released material was mostly xenon, and small amounts of iodine and cesium.

Lorenz⁴³ recently reviewed fission product release data for aluminum-uranium alloys. Studies were done in helium, air and steam. From the studies, it was determined that oxidation increases iodine and tellurium releases, that U_3O_8 fuel releases iodine and cesium at lower rates than UAl alloy, and that the melting point of the matrix affects release rate. Good agreement was obtained between data from Parker⁴⁴ and HEDL⁴⁵ except for the cesium release rate.

Whitkop⁴⁶ summarized experiments done at Hanford Engineering Development Laboratory using SRP irradiated aluminum-uranium alloy fuel and U_3O_8 -Aluminum dispersion fuel⁴⁷. In general, the effect of fuel temperature had a greater effect on the amount of fission product release than atmosphere.

The fuel melting experiments indicated that a 100% release of the iodine inventory in the melted portion of the core was likely in the event of core damage. Experimental uncertainty in the post-melt iodine chemistry made it difficult to state what percentage of the released iodine reached the carbon filter. There was evidence to suggest that under some circumstances, a significant fraction of the released iodine can react with condensed phases of cesium to form cesium iodide via surface reactions. In the presence of water vapor, some of the released iodine may be in the form of hydrogen iodide.

All of the noble gas inventory contained in the melted portion of the core was released. Krypton-85 was released irrespective of the atmosphere, as long as the

fuel remained above its melting point. All noble gases were probably released within 45 seconds after the fuel melted. Cesium produced particulates upon encounter with a relatively cooler atmosphere. The bulk of the cesium was in elemental form, but some reacted with steam to form cesium hydroxide. The atmosphere had a measurable effect on cesium release, temperature had a greater effect.

A second series of experiments was done at HEDL⁴⁸. Higher melt temperatures, up to 1000°C, were used in this experiment. A summary of the results was reported by Whirkop⁴⁹.

Pre-melt measurements of the gamma-active fission products showed good agreement with previous measurements. The fission product release fractions were in reasonable agreement with earlier ORNL data on U/Al fuel melts. A comparison of ORNL and SRL data for iodine release is shown in Figure 21. Data was taken using U-Al coupons.

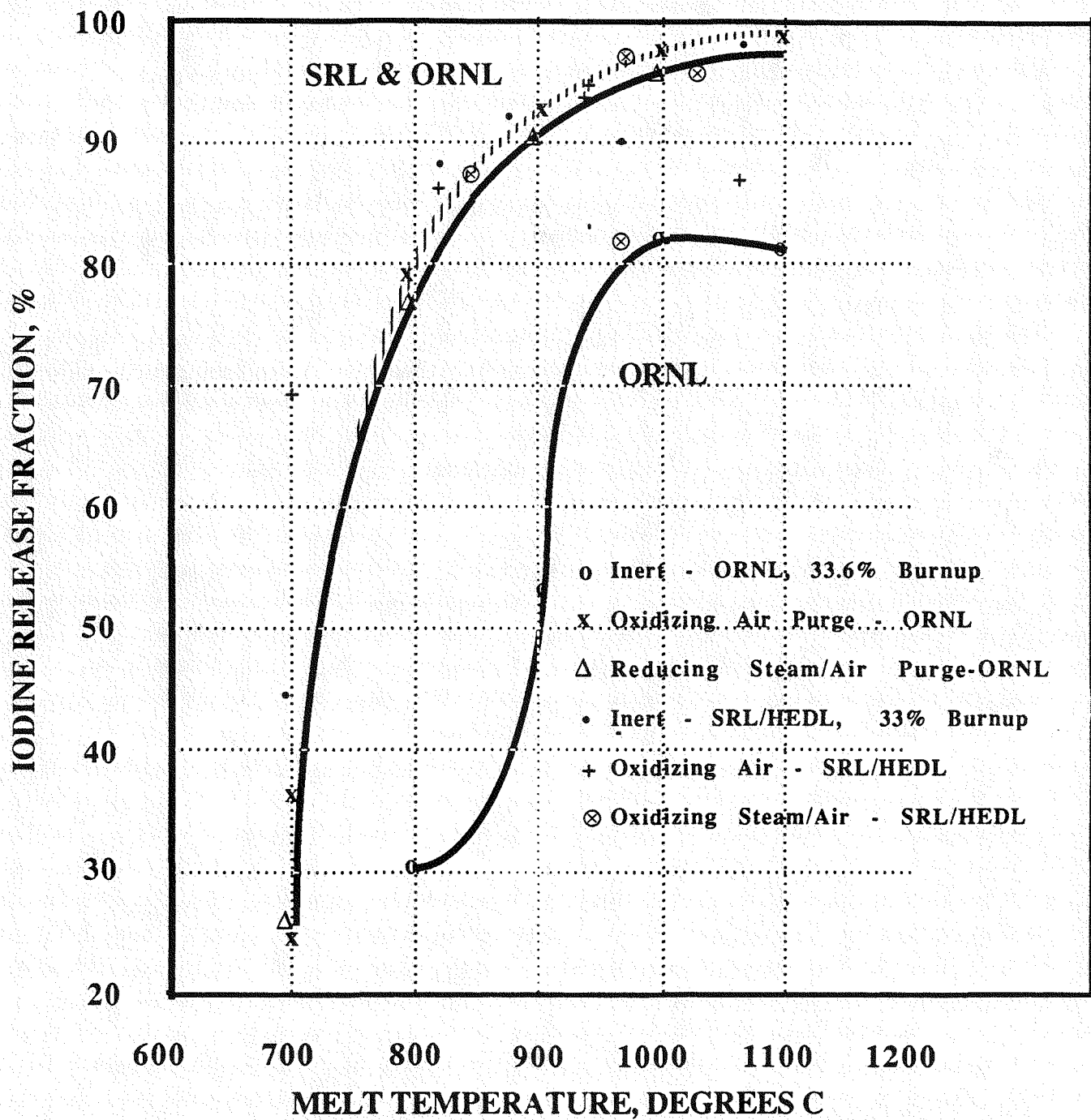


FIGURE 21. COMPARISONS OF ORNL AND SRL DATA FOR U-AI COUPON IODINE RELEASE

REFERENCE: Whittrop, P.G., "Summary of the Second Series of SRL Fuel Melt Experiments," E. I. de Pont de Nemours & Co., DPST-87-412, July 23, 1987.

7.0 FABRICABILITY

7.1 Casting

Differences in the density of primary phases and the liquid can lead to alloy segregation during casting. The density of the intermetallic compounds vary from about 5.7 to 6.8 gm/cc while the density of molten aluminum is less than 2.7 gm/cc. Gravity segregation of aluminum-uranium alloys containing up to 45 wt% uranium has been studied by several investigators^{50,51,52,53}. Severity increases with increase in uranium content. Rotation of the mold during pouring and solidification of the cast alloy is used at SRS to reduce alloy segregation. The billet core is also made up of several individual castings which are assembled in a manner to reduce axial fuel variations in the final extruded tube.

7.2 Fuel Density Limit

Extrusion tests given in Table X were done at SRS to define the upper limit for the manufacture of reactor fuel tubes^{54,55}. The uranium content ranged from 35 to 45 wt%. Both single and double extrusion processes were evaluated. Standard production conditions were used along with "improved" conditions.

The yield data are plotted in Figure 22. The extrusion yield was 100% at 35 wt% uranium which was determined by extruding less than 100 tubes. As the uranium content increased the yield decreased for both single and double extrusion operations. Double extrusion gave a much lower yields although the ductility is reported to increase with prior hot working¹⁶. Using "improved extrusion conditions" the yield at 40 wt% uranium was 100% for 61 extruded tubes.

When combining extrusion with other metal working operations, the overall yield for the manufacture of reactor fuel tubes with greater than about 35 wt% uranium is expected to be significantly lower than current yields for aluminum-uranium alloys.

7.3 Tube Fabrication and Production Yields

Fuel tubes are manufactured in the 321-M Building. U-Al billets are cast and extruded to form logs. The logs are machined into co-extrusion billet cores and then extruded a second time to produce aluminum fuel tubes. Since the mid 70's, this double extrusion process has been used to make reactor fuel tubes for the Savannah River Reactors.

The 321-M Building has a casting area, billet assembly area, extrusion area, inspection and finishing area, and offices and shops. Figure 23 provides a process flow diagram for the process summarized below.

Alloy Preparation in Ingot Casting

High purity aluminum ingots, high enriched uranium metal, and U-Al scrap are blended to a uniform U-235 concentration, based on available U-235 and desired fuel tube loading. Melting and alloying are conducted in graphite crucibles. The alloy is then cast into graphite molds to form hollow, cylindrical ingots. The ingots are machined in preparation for assembly into pre-extrusion billets.

TABLE X
EXTRUSION YIELDS OF HIGH URANIUM
CONCENTRATION MARK 16 OUTER TUBES

<u>Wt. % U</u>	<u>Extrusion Process</u>	<u>Extrusion Conditions</u>	<u>Number of Tubes</u>	<u>Yield* %</u>
35	Single	Standard	38	100.0
35	Double	Standard	73	100.0
40	Single	Standard	46	91.5
40	Double	Standard	65	57.5
45	Single	Standard	8	62.5
45	Double	Standard	20	5.0
40	Double	Improved	61	100.0
45	Double	Improved	31	0.0

* Yields do not consider other steps in the tube fabrication process.

** Improved Extrusion conditions relate to lower extrusion ratio, billet preheat temperature and tooling temperature.

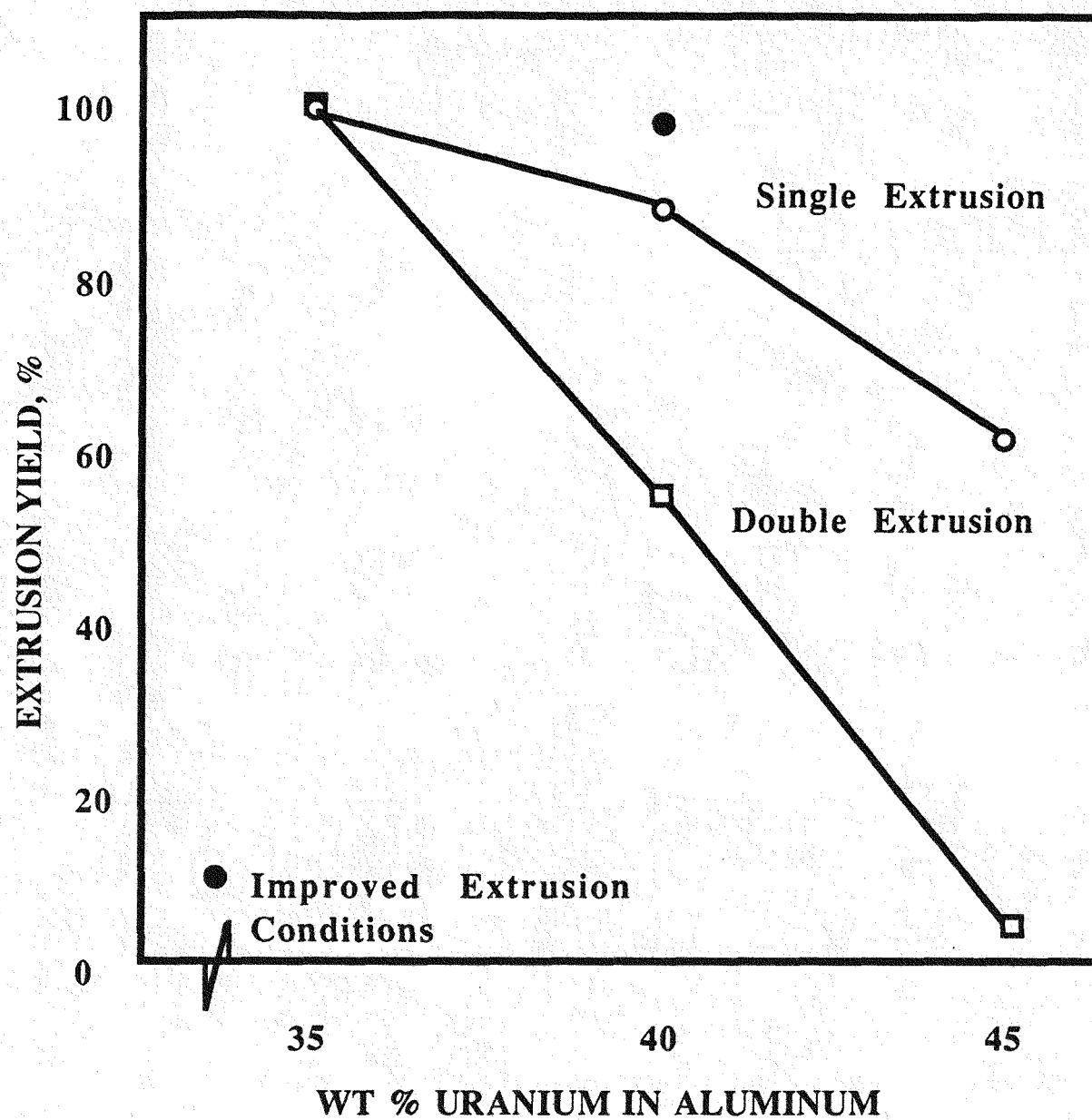


FIGURE 22. EXTRUSION YIELDS FOR HIGH WT % URANIUM-ALUMINUM

REFERENCE: Hester, J.R., Raw Materials Works Technical Monthly Report, DPSP-79-71-16, 1979

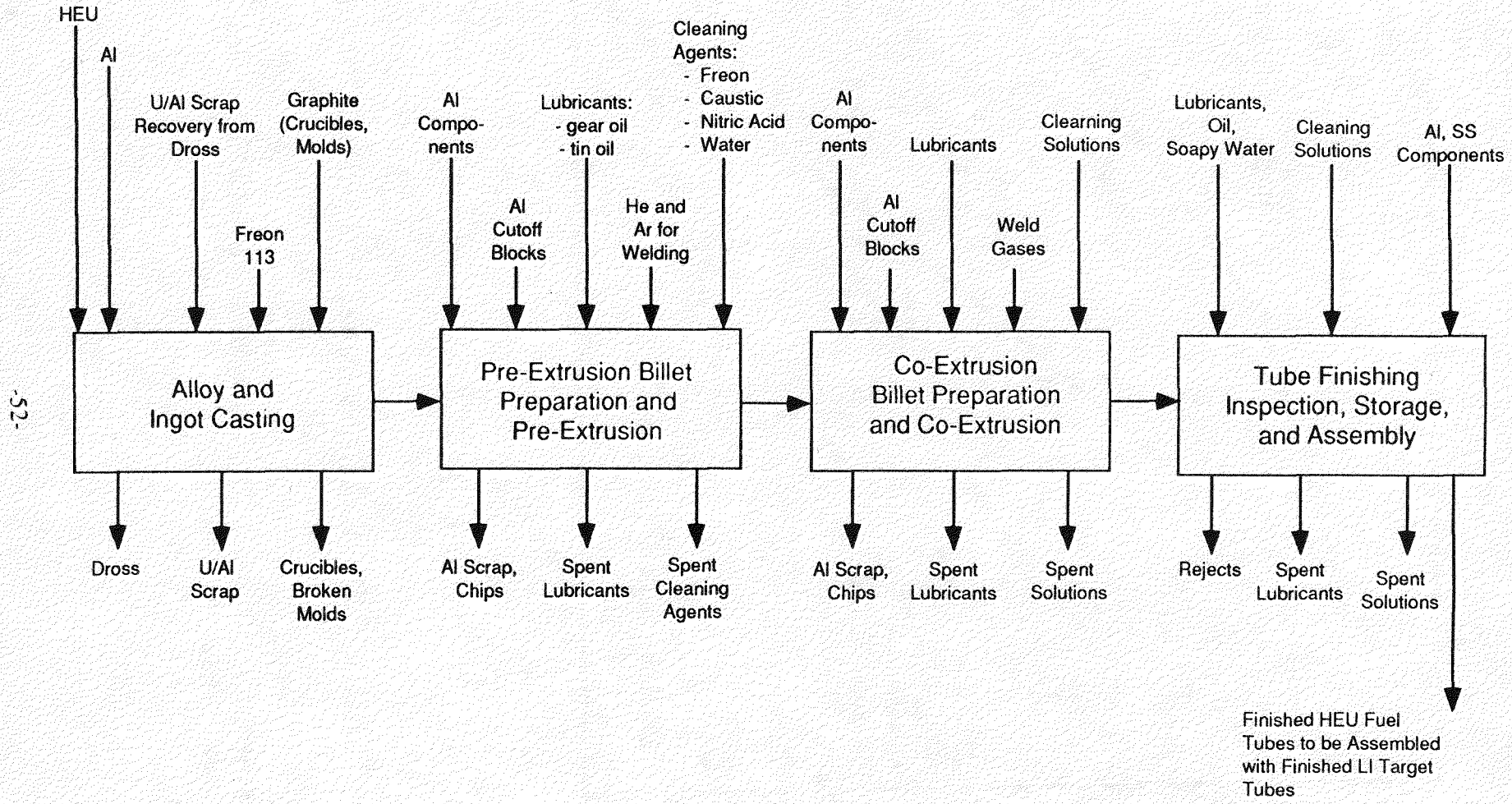


FIGURE 23. FLOW DIAGRAM FOR HWR FUEL TUBE FABRICATION PROCESS

Pre-extrusion Billet Preparation and Pre-extrusion

Machined Al-U alloy cores are concentrically assembled into a composite pre-extrusion billet. Clean aluminum outer and inner sheaths and end plugs are placed around the cores and welded together to encapsulate the cores and provide for containment for the U-Al alloy throughout the remaining process steps. The billet is heated and outgassed prior to pre-extrusion. Pre-extrusion produces aluminum-clad hollow tubular logs which, after cleaning, cutting, machining and inspection, will become co-extrusion billet cores in the following step.

Co-extrusion Billet Preparation and Co-extrusion

Co-extrusion billets are prepared in a similar manner as the pre-extrusion billets. Billet cores are encapsulated in aluminum components whose external joints are welded. Billets are heated and outgassed to remove air and volatile contaminants. Graphite based lubricants and powdered tin/oil lubricants are used in the extrusion process. The fuel tubes are formed and aluminum cladding and end plugs are metallurgically bonded to the cores during co-extrusion.

Tube Finishing, Inspection, Storage, and Assembly

The fuel tube is degreased using Freon, nitric acid, caustic and process water rinses. A thermal test is performed to detect the presence of gas pockets in the extruded material. Any tubes rejected in this step are recycled in the melt/cast operation. Tubes are cold drawn, using a gear oil lubricant, to produce accurate final dimensions and provide for improved surface finish. The tubes are then straightened on a rolling mill, and degreased and machined prior to final inspection and storage. In subassembly, three finished tubes are nested in a soapy water bath (for lubrication) to form the fuel portion of the assembly. Final assembly will be accomplished when two target tubes are added, one positioned inside and the other outside the fuel tube subassembly. End fittings are attached by Magneforming (a non-contacting electromagnetic joining process).

The maximum uranium content of aluminum-uranium fuel elements at SRS has increased over the years and is currently 33 wt%. Each type tube in the assembly has a different uranium content which is determined during charge makeup.

The overall tube fabrication yield for the past 7 years is shown in Figures 24 and 25 for Mark 16 and Mark 22 type fuel tubes. The overall yield for Mark 16 tubes has averaged about 78% while the average overall yield for Mark 22 tubes has slightly increased from about 80% in 1979 to about 85% in 1986.

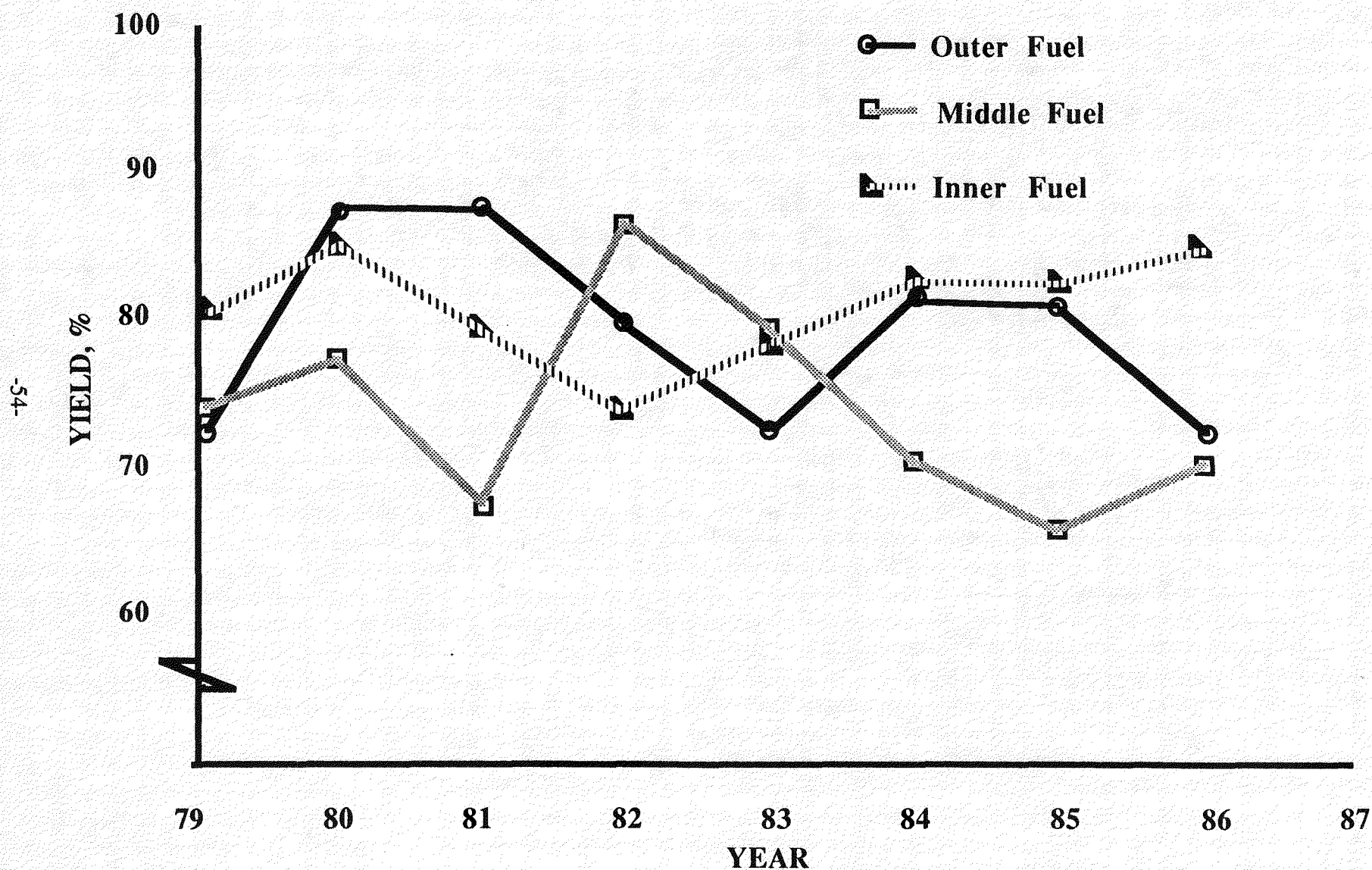


FIGURE 24. MARK 16 FUEL PRODUCTION YIELD DATA FOR 1978 - 1986

Reference: Raw Materials Monthly reports, E.I. duPont de Nemours & Co., 1979-1986

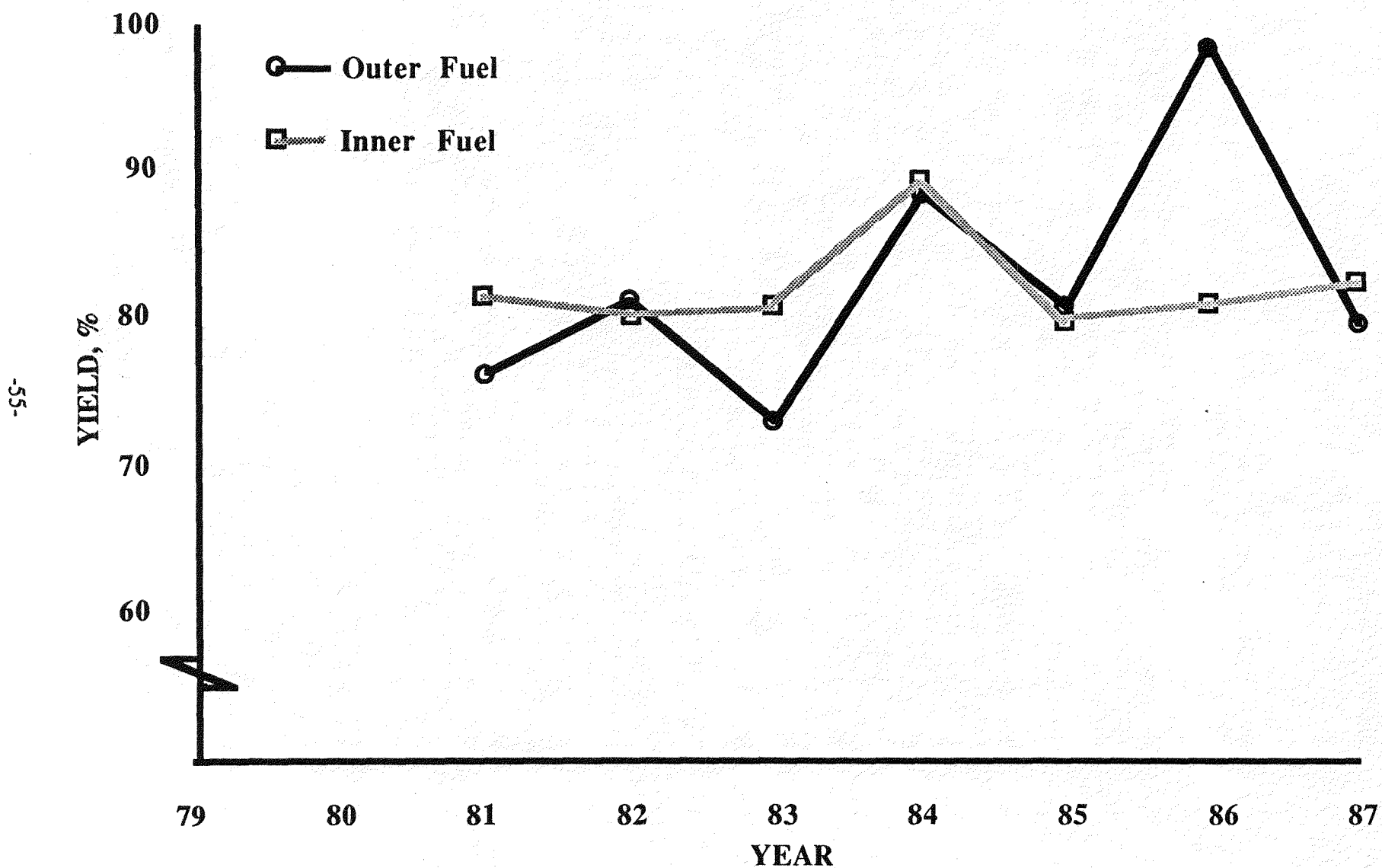


FIGURE 25. MARK 22 FUEL PRODUCTION YIELD DATA FOR 1979 - 1987

Reference: Raw Materials Monthly Reports, E.I. duPont de Nemours & Co., 1980-1987

8.0 REPROCESSING

8.1 Physical Description

The spent fuel at the Savannah River Site is highly enriched uranium fuel that has been irradiated in the reactors. These spent fuel assemblies are processed to recover uranium, neptunium and plutonium.

The processing of radioactive material occurs in the two canyons. All equipment that handles potentially highly radioactive materials is located in one of two parallel longitudinal building sections designated the Hot Canyon and Warm Canyon, respectively, to indicate the radiation intensities of the materials being processed.

8.2 Process Description

The H-Canyon facility uses the HM process to separate uranium, neptunium, and fission products. Irradiated uranium fuels containing U-235 at enrichments from 1.1% to 94% are processed and the uranium recovered and converted to a solid form along with neptunium. Before being processed, the irradiated fuels are aged about 200 days to allow short-lived radionuclides such as I-131 to decay. There are three major operations associated with the operation of the H canyon complex. These are: 1) fuel dissolution and clarification where the metal fuel is dissolved and the resulting solution treated to remove suspended particulates, 2) solvent extraction where the metal solution is processed to recover and then purify uranium and neptunium, and 3) product conversion where the various purified nitrate streams are converted from a liquid to a solid form. Each of these are briefly discussed in the following paragraphs.

DISSOLUTION AND CLARIFICATION

In the HM process, aluminum-clad fuels are dissolved in nitric acid using a mercury catalyst. The dissolution rate is controlled to limit the rate of off-gas generation. The dissolved solutions are concentrated and then treated with gelatin to remove silica. After the solution has been treated with the gelatin, it is then processed through a centrifuge to produce a solids-free solution.

All processing steps for spent fuel have been demonstrated by production plant operations over a long period of time.⁵⁶ Without question, the technology basis for processing LTHWR fuel is firmly established. Processing of aluminum-clad fuels with an aluminum-uranium alloy core has been a standard operation at SRS for over 30 years.

SOLVENT EXTRACTION

Separation of uranium and neptunium from fission products and from each other is accomplished by multistage solvent extraction with tri-n-butyl phosphate (TBP) in kerosene. A series of extraction and stripping steps are used to accomplish the separation and purification. There are adjustments in the concentration and chemistry of the solution between the steps to assist in the extraction and stripping operations. The solvent extraction operation produces purified nitrate streams of uranium and neptunium as well as a high level waste stream that contains most of the fission products that were present in the irradiated fuel and low level aqueous waste streams such as condensed evaporator overheads.

PRODUCT CONVERSION

The purified nitrate streams produced by the solvent extraction operation are converted to the solid forms. The uranium is converted from the nitrate form to the oxide form by a process where the uranium nitrate is evaporated and then thermally denitrated to form UO_3 .

The neptunium and plutonium nitrate solutions are converted to oxides in the HB line. The HB-line is located on top of the 221-H Building on the fifth and sixth levels. Only one portion of the HB-line will be used in the processing of NPR fuel.

The Neptunium Oxide Facility converts neptunium nitrate solutions to oxide powder. The process consists of feed receipt and adjustment, anion exchange, concentration, neptunium oxalate precipitation, filtration, drying, and calcination of the oxalate cake to oxide.

The plutonium nitrate solutions associated with processing NPR fuel will not be treated to recover the small amount of plutonium but will be combined with the high level liquid waste stream.

Figure 25 is a flow diagram summarizing the processing of irradiated fuel to NpO_2 , and UO_3 .

8.3 Waste

Liquid wastes from processing aluminum-based fuels have been stored primarily in alkaline form in carbon steel tanks. There also is experience with acidic waste in stainless steel tanks. Liquid waste has been calcined to give a granular refractory solid, and much experience for this is available at the Idaho Chemical Processing Plant. Proposed treatment of the long-stored neutralized waste at SRS takes advantage of the natural in-tank segregation, to a sludge, of metal hydroxides that carries almost all the fission radioisotope products, and a supernate in which cesium is the primary radioisotope remaining. The supernate is further decontaminated by an in-tank precipitation process that removes cesium and residual amounts of other radionuclides.

The final result of in-tank operations are (1) a decontaminated salt solution that is solidified as concrete low-level waste, (2) a concentrate that contains over 99.99% of the cesium from the salt, and (3) a washed sludge. The latter two are further processed in the vitrification plant, combined, and vitrified in a borosilicate glass. All in-tank processes have been demonstrated at full scale in actual SRS waste tanks. All vitrification plant processes have been demonstrated with actual waste samples at laboratory scale. Vitrification and off-gas decontamination equipment up to two-thirds equipment size giving 44% of the required production rate, has been operated with nonradioactive, simulated waste.

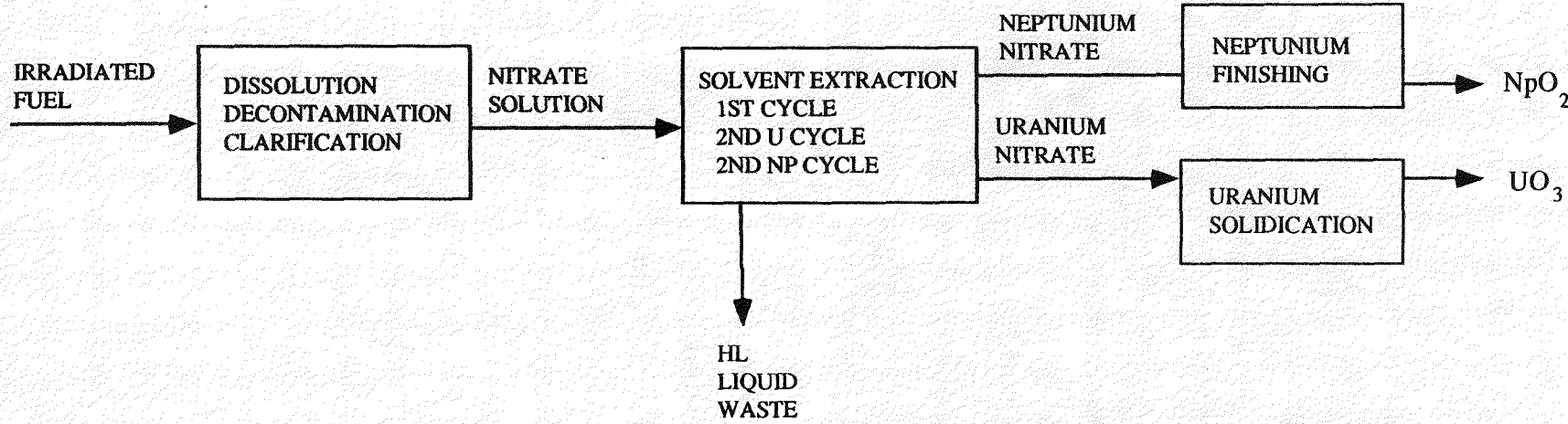


FIGURE 26. FLOW DIAGRAM FOR PROCESSING IRRADIATED FUEL TO NpO_2 AND UO_3 (H AREA)

REFERENCES

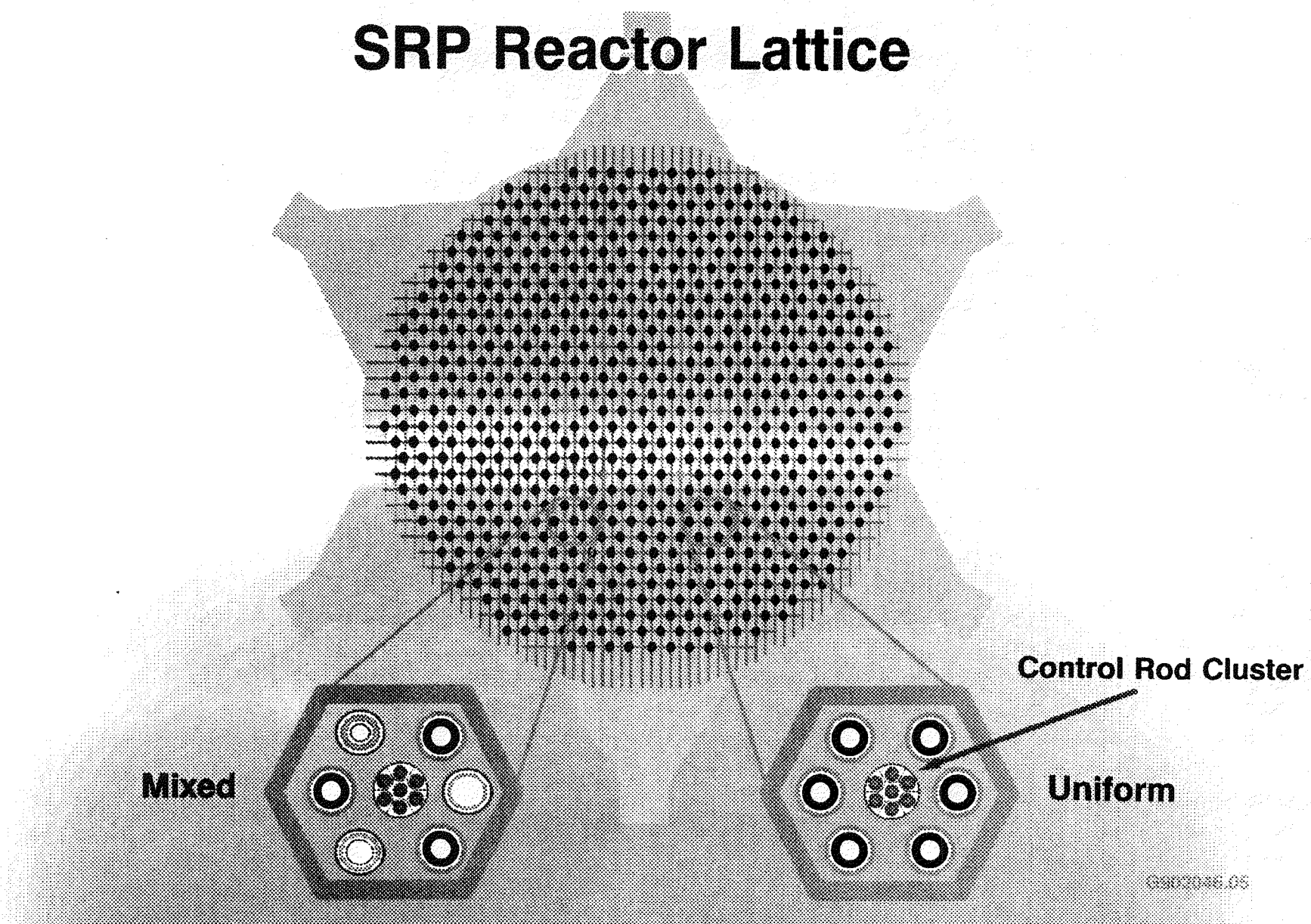
1. Binary Alloy Phase Diagrams, Massalski, T. B.(editor in chief), Am.Soc. for Metals, x, 1986.
2. Gordon, P. and Kaufmann, A. R., AIME Trans., 188, p 182, 1950.
3. Jones, T. I., McGee, I. J. and Norlock, L. R., At. Energy Can. Ltd., AECL-1215, p29, 1961.
4. Jones, T. I., Street, K. N., Scoberg, J. A. and Baird, J., "Relationship Between Microstructure and Thermal Conductivity in Aluminum-Uranium Alloys," Can. Met. Quart., V2, pp 53-72, 1963.
5. Mondolfo, L. F., Aluminum Alloys: Structure and Properties, Butterworth & Co. (Publishers) Ltd., London, 1976.
6. Thurber, W. C. and Berver, R. J., "Development of Silicon-Modified 48 Wt% U-Al Alloys for Aluminum Plate-type Fuel Elements," ORNL-2602, 1955.
7. Borie, B. S., "Crystal Structure of UAl₄", J. of Metals (Trans. AIME), 3, pp 800-802, 1951.
8. Gordon, P. and Kaufman, Op. Cit, 182
9. Aronin, L. R. and Klein, J. L., "Use of a Density (Specific Volume) Method as a Sensitive Absolute Measure of Alloy Composition, and Its Applications to the Aluminum-Uranium System," Nuclear Metals, Inc., NMI-1118, 1954.
10. Saller, H.A., "Preparation, Properties, and Cladding of Aluminum-Uranium Alloys," in Proceedings of the International Conference on the Peaceful Uses of Atomic Energy, Vol 9, P/562, p 214, United Nations, New York, 1956.
11. Hunter, L. P., "Thermal Conductivity of Uranium-Bearing Material under Irradiation at High Temperatures," J.of Metallurgy and Ceramics(secret), Issue No. 2, p. 41, Jan. 1949.
12. Billington, Douglas, and Crawford, Jr., J. H., Radiation Damage in Solids, Princeton University Press, p389, 1961.
13. Faris, F. E., "A compendium of Radiation Effects on Solids," NAA-SR-241, Vol. 1, p. 120, Issued Oct. 6, 1953.
14. Marchiden, D. I. and Ciopes, M., "Enthalpy of Uranium to 1500 K by Drop Calorimetry," J. Chem Thermodynamics, 8,
15. Chiotte, P. and Kateley, J. A., "Thermodynamic Properties of Uranium-Aluminum Alloys", J. of Nucl. Mat., 32, pp 135-145, 1969.
16. Gimpl, M. L. and Huntoon, R. T., "Properties of Aluminum-Uranium Alloys Containing 16 to 45 Per Cent Uranium," E. I. du Pont de Nemours & Co., DP-256, 1957.

17. Gibson, G. W., Graber, M. J., Beeston, J. M. and Porter, E. H., "Mechanical Property Measurements," in Materials Testing Reactor-Engineering Test Reactor Technical Branches Quarterly Report, January 1-March 31, 1962, Phillips Petroleum Company, Atomic Energy Division, p 10, IDO-16781, June 15, 1962.
18. Bowen, H. C. and Dillion, R. L., "Integranular Corrosion of Al-U and Al-Si-U Alloys," Hanford Atomic Products Operation, HW-55352, March 14, 1958.
19. Ruther, W. E. and Draley, J. E., "Corrosion of Al-U Alloys in High Temperature Water," Argonne National Laboratory, ANL-6054, 1959.
20. Daniel, N. E., Foster, E. L., DeMastry, J. A., Bauer, A. A. and Dickerson, R. F., "Study of Aluminum Alloys Containing up to 45 w/o Uranium," Battelle Memorial Institute, BMI-1183, April 30, 1957.
21. Argonne National Laboratory, Studies of Preirradiated Fuels in TREAT, p 94, ANL-6912, 1964.
22. Argonne National Laboratory - Reactor Development Program Progress Report, p 72, ANL-6880, 19XX.
23. Argonne National Laboratory - Reactor Development Program Progress Report, p 97, ANL-6860, 1964.
24. Martinson, Z. R., "Survey of Literature on Particle Size, Surface Area, Oxidation and Pressure Generation after Uranium - Aluminum core Melt," PG-T-89-003, 1989.
25. Morin, J. P. and Hyder, M. C., "The Reaction of Molten SRP Reactor Fuel with Water," E. I. du Pont de Nemours & Co., presented at ANS Workshop on the Safety of Uranium- Aluminum Fueled Reactors, Idaho, 1989.
26. Morin, J. P. and Hyder, M. L., "The Reaction of Molten SRP Reactor Fuel with Water," Presented at ANS Workshop on the Safety of Uranium-Aluminum Fueled Reactors, Idaho, 1989.
27. Kittel, J. H., Gavin, A. P., Corthers, C.C. and Carlander, R., "Performance of Aluminum-Uranium Alloy Reul Plates Under High Temperature and High Burnup Conditions," Argonne National Laboratory, ANL-FGF-392 (TID-7642), 1962.
28. Caskey, G. R. and Angerman, C.L., Swelling of Mark VIJ Fuel, E. I. du Pont de Nemours & Co., DPST-65-259, August 30, 1962.
29. Angerman, C. L., E. I. du Pont de Nemours & Co., Laboratory Notebook, DPSTN-1468(Secret), pp.144-150, 1961.
30. Hofman, G. L., "Fission Gas Bubbles in Uranium Aluminide Fuels," Nuclear Technology, Vol. 77, p. 110, Apr. 1987.
31. WASH-296
32. Argonne National Laboratory-Reactor Development Program Progress Report for December 1961, Irradiation Studies, ANL-6485, p 7, 1961.

33. Caskey Jr., G. R. and Angerman, C. L., "Swelling of Irradiated Al-U Alloy During Postirradiation Annealing," E. I. du Pont de Nemours & Co., DPST-65-351, July 13, 1965.
34. Brookhaven National Laboratory, Nuclear Engineering Department Progress Report, September-December 1961, USAEC Report BNL-705, p. March 1962.
35. Gavin, A. P. and Crothers, C. C., "Irradiation of an Aluminum Alloy-Clad, Aluminum-Uranium Alloy-Fueled Plate," Argonne National Laboratory, ANL-6180, July 1960.
36. Ivins, R. O., "A Study of the Reaction of Aluminum/Uranium Alloy Fuel Plates with Water Initiated by a Destructive Reactor Transient," Trans. Am. Nucl. Soc., 6, pp 101-2, 19XX.
37. Seaboch, J. R. and Wade, J. W., "Fuel Meltdown Experiments," E. I. du Pont de Nemours & Co., DP-314, Oct. 1958.
38. Harpring, J. R., "Inspection of Irradiated Mark 18 Fuel Tubes," E. I. du Pont de Nemours & Co., DPSP-70-1096, 1970.
39. Harpring, J. R., "Inspection of Irradiated Mark 22 Fuel Tubes," E. I. du Pont de Nemours & Co., DPSP-73-1167, 1973.
40. Rankin, W. N., "Cladding Penetrations in Irradiated Al-U Fuel Tubes," E. I. du Pont de Nemours & Co., DP-1350(Secret), September, 1974.
41. Hyder, M. L. and Parks, P. B., "Severe Accident Analysis for the NPR-HWR: Bounding Thermodynamic Calculations," E. I. du Pont de Nemours & Co., DPST-88-383, April 1988.
42. Shibata, T., Tamai, T., Hayashi, M., Posey, J. C. and Snelgrove, J. L., "Release of Fission Products from Irradiated Alumide Fuel at High Temperatures," Nuclear Science and Engineering: 87, 405-417, 1987.
43. Lorenz, R. A., "Fission Product Release Experiments," Oak Ridge National Laboratory, Presented at the ANS Workshop on Safety of Uranium-Aluminum Fuel Reactors, March 15, 1989.
44. Parker, G. W., Barton, C. J., Creek, G. E., Martin, W. J., and Lorenz, R. A., "Out-of-pile Studies of Fission-Product Release from Overheated Reactor Fuels at ORNL," Oak Ridge National Laboratory, ORNL-3981, 1967.
45. Woodley, R. E., "The Release of Fission Products from Irradiated SRP Fuels at Elevated Temperature," HEDL-7598, June 1986.
46. Whitkop, P. G., "Summary Report on the Release of Fission Products from Irradiated SRP Fuel at Elevated Temperatures," E. I. du Pont de Nemours & Co., DPST-86-406, April 21 1986.
47. Woodley, R. E., OP Cit.
48. Woodley, R. E., OP Cit.

49. Whitkop, P. G., "Summary of the Second Series of SRL Fuel Melt Experiments," E. I. du Pont de Nemours & Co., DPST-87-412, July 23, 1987.
50. Allen, B. C. and Isserow, S., "Segregation at the Eutectic Temperature," *Acta Metallurgica*, Vol. 5, p 465, 1957.
51. Bramfitt, B. L., and Leighly, Jr., H. P., "A Metallographic Study of Solidification and Segregation in Cast Aluminum-Uranium Alloys," *Metallography*, 1 pp 165-193, 1968.
52. Thruber, W. C. and Beaver R. J., "Segregation in Uranium-Aluminum Alloys and its Effect on the Fuel Loading of Aluminum-Base Fuel Elements," Oak Ridge National Laboratory, ORNL-2476, Sept. 1958.
53. Daniel, N. E. Foster, E. L., DeMastry J. A., Bauer A. A. and Dickerson R. F., "Study of Aluminum Alloys Containing up to 45 wt% Uranium," Battelle Memorial Institute, BMI-1183, April 1957.
54. Rhode, F. C., "Fuel Tube Core Concentration and Expected Fabrication Yields," E. I. du Pont de Nemours & Co., DPSP-82-71-4, February 16, 1982.
55. Hester, J. R., Raw Materials Works Technical Monthly Report, E. I. du Pont de Nemours & Co., DPSP-79-71-16, 1979.
56. Spent Fuel Processing in Support of the New Production Reactor, Prepared for the U.S. Department of Energy under Contract DE-AC06-77R6L01030, Rockwell International, Rockwell Hanford Operations, Section 4 and Appendix A, RHO-RE-EV-47, August 1984.

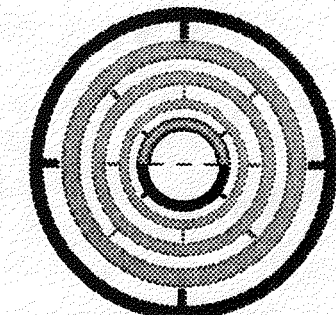
SRP Reactor Lattice



APPENDIX 1

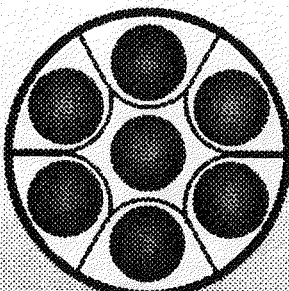
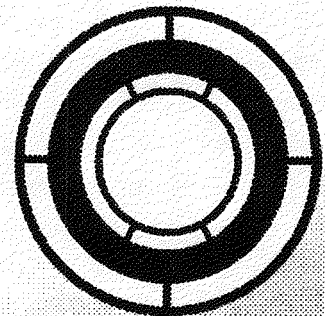
Mixed Lattice

MK-16

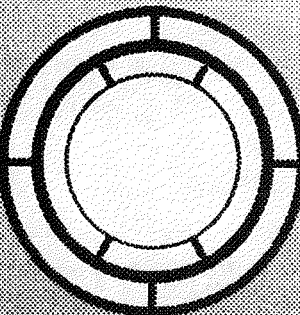
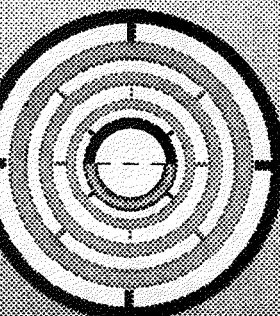


MK-30A

MK-30B



MK-16

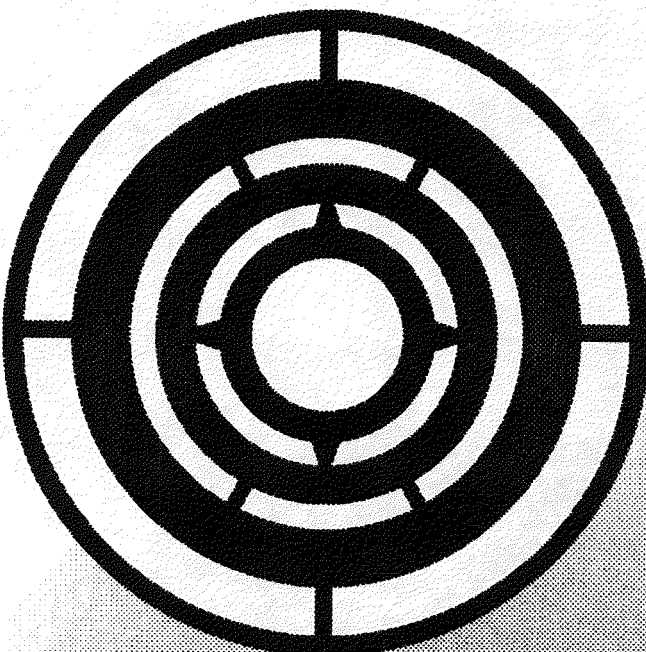


MK-16

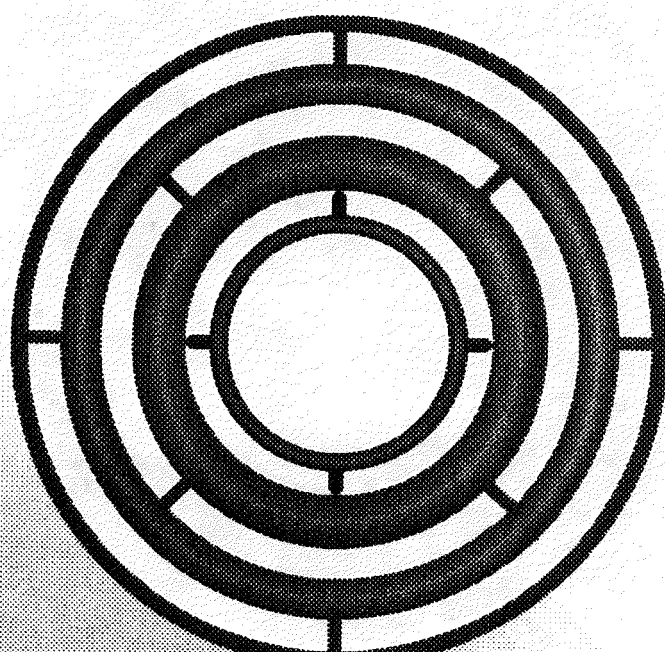
MK-30C

0302036.09

Low Enriched Uranium Slug Assemblies



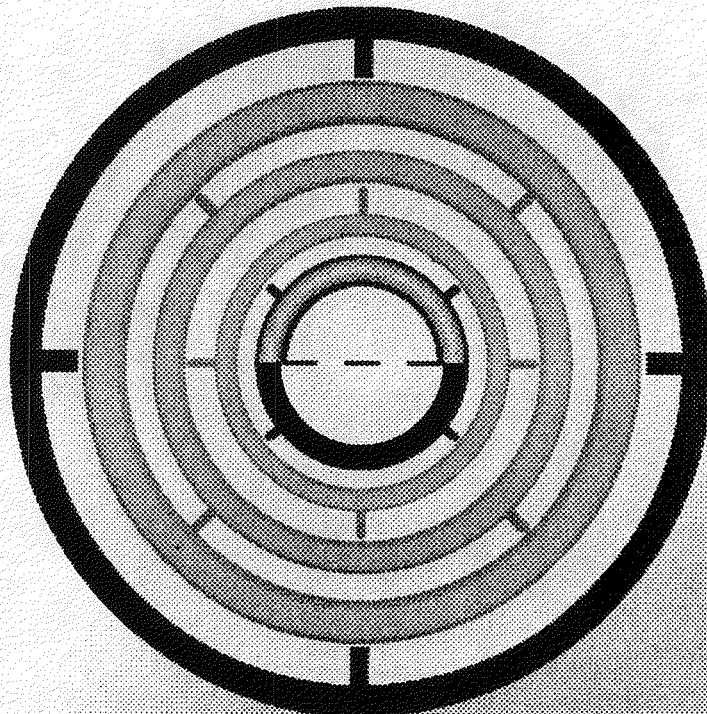
**MK-31 A, B Slugs
(Depleted U)**



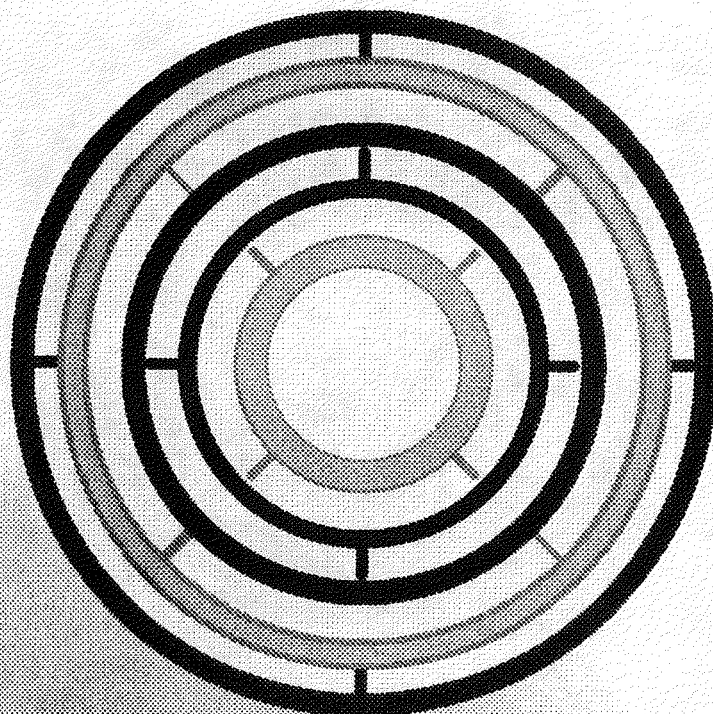
**MK-15 (Slugs)
(1.1% U-235)**

0002046.07

High Enriched Uranium Tubular Assemblies



MK-14 and 16 (Tubes)
(58-93% U-235)



MK-22 (Tubes)
(65-93% U-235)

0302046.08